Hydrological Sciences Journal

ISSN: (Print) (Online) Journal homepage: https://www.tandfonline.com/loi/thsj20

# Innovative approaches to the trend assessment of streamflows in the Eastern Black Sea basin, Turkey

Fatma Akçay, Murat Kankal & Murat Şan

**To cite this article:** Fatma Akçay, Murat Kankal & Murat Şan (2022) Innovative approaches to the trend assessment of streamflows in the Eastern Black Sea basin, Turkey, Hydrological Sciences Journal, 67:2, 222-247, DOI: 10.1080/02626667.2021.1998509

**To link to this article:** https://doi.org/10.1080/02626667.2021.1998509

Published online: 18 Jan 2022.

HYDROLOGICAL SCIENCES JOURNAL
2022, VOL. 67, NO. 2, 222–247
https://doi.org/10.1080/02626667.2021.1998509



# Innovative approaches to the trend assessment of streamflows in the Eastern Black Sea basin, Turkey

Fatma Akçay [a], Murat Kankal [a] and Murat Şan [b]

[a]Civil Engineering Department, Bursa Uludağ University, Bursa, Turkey; [b]Civil Engineering Department, Gümüşhane University, Gümüşhane, Turkey

**ABSTRACT**

The issue of detection of hydrometeorological trends remains relevant because of the importance of climate change in design, operation, and management studies related to water resources. This study examines the effects of changes in climate and land use on monthly flows (1962–2018) in the Eastern Black Sea basin, Turkey, using innovative trend analysis methods. In this context, innovative polygon trend analysis (IPTA) and innovative trend significance test (ITST) were used to detect the trends and compared with Mann-Kendall test. Only stations with homogeneous data that did not experience non-climatic changes are used in the analysis. IPTA and ITST approaches are much more sensitive than Mann-Kendall in detecting trends. Although the innovative methods are mostly compatible with each other (90%), IPTA presents additional information about trend transitions between successive parts of time series. Results indicate significant decreasing trends in summer months, likely due to diminishing precipitation and effective evaporation.

**ARTICLE HISTORY**
Received 25 December 2020
Accepted 23 September 2021

**EDITOR**
S. Archfield

**ASSOCIATE EDITOR**
K. Ryberg

**KEYWORDS**
trend analysis; innovative trend significance test; innovative polygon trend analysis; Mann-Kendall test

## 1 Introduction

In the 5th Assessment Report of the Intergovernmental Panel on Climate Change (IPCC 2013), it was announced that the global average temperature increased by 0.89°C between 1901 and 2012. It has been determined that due to fossil fuel use and land-use changes, carbon dioxide emission increased by 40% compared to the pre-industrial revolution period (IPCC 2013). In addition, many changes have occurred in extreme weather and climate events since 1950. It is predicted that changes in precipitation, one of the most significant of these events, will continue. It is forecasted that the increase in global temperatures will probably exceed 1.5°C by the end of the 21st century. It has been proven that the climate change we are experiencing is likely due to human influence (IPCC 2013). As stated in the IPCC (2013) report, it is clear that climate change continuously affects hydrometeorological processes. These effects make themselves conspicuous in the form of trends or unexpected shifts (Şen 2014).

Climate change and land-use change are generally considered two of the main contributing factors to changes of the hydrological cycle (Tan *et al.* 2015). Especially in large river basins, two possible causes of flow changes are precipitation variability and land-use changes (Costa *et al.* 2003). Climate variability impacts flow volume, peak flow, and flow routing time (IPCC 2007, Kundzewicz *et al.* 2008, Li *et al.* 2009, Tan *et al.* 2015). Land-use changes, in turn, influence surface runoff, flood frequency, and annual mean flow (Huntington 2006, Brown *et al.* 2013, Wei *et al.* 2013, Tan *et al.* 2015). Flow is one of the most important parameters considered in the management of water resources. Flow measurement is an essential step in projects that will be carried out depending on energy production potential and drinking/utility water capacity in a stream (Ay and Kişi 2017). In addition, flow data are considered in the design of important water storage areas such as flood protection structures and dams (Cigizoglu *et al.* 2005). Therefore, it is important to understand the change in flow data over time.

Examination of historical flow data can reveal trends that are potentially related to climate change or land-use change. Predicting future changes, especially in regions where significant changes are experienced, can be enhanced by using scenarios. In addition, as a traditional approach, engineering structures are not designed with the inclusion of increasing or decreasing trends under climate change. However for reliable calculations, these should be included in climate change risk calculations. There are studies on how trend analysis results can be included in risk calculations (Rosner *et al.* 2014, Almazroui *et al.* 2019, Şen 2020). Therefore, trend analysis is important for planning.

It is predicted that temperatures will increase and precipitation will decrease in the Mediterranean basin, stretching from Cabo Verde in the west to Jordan and Turkey in the east and from Italy in the north to Tunisia in the south (IPCC 2013). In this regard, Turkey is situated in a sensitive geographic area in terms of climate change. Turkey is divided into 26 hydrological basins; among them, the Eastern Black Sea basin (EBSB) with 753 mm mean flow height is the third largest basin with the maximum total flow rate (9.5%) after the Tigris and Euphrates basins. Furthermore, with an annual average rainfall of 1198 mm, the EBSB is the catchment with the highest rainfall in Turkey (Odemis and Evrendilek 2007, Satılmış 2015). The basin receives rainfall in all seasons and has significant hydroelectric potential due to its streams with steep slopes. The annual hydroelectric energy potential of the basin is 10 944 GWh. With 2790 MW of installed power facilities, the EBSB contributes

**CONTACT** Fatma Akçay fatmaakcay93@gmail.com

9.9% of the total facilities in operation in Turkey as of 2018 (Kankal and Akçay 2019a). The EBSB is frequently exposed to floods due to its topographical structure, extreme precipitation, and snow melting in the spring months (Yüksek *et al.* 2013). Increasing trends have been observed in the rainfall intensity in the basin (Nemli 2017).

Trend analysis methods are divided into parametric and nonparametric methods. Parametric methods are grounded on the assumption that the data fit a normal distribution. Since the data do not need to fit a normal distribution in nonparametric methods, these methods are generally preferred in trend analysis studies (Onyutha 2016). Mann-Kendall test, Spearman's rho test, and Sen's trend slope test are some examples of nonparametric methods. Mann-Kendall test is commonly used in studies (Zhang *et al.* 2008, Saplıoğlu *et al.* 2014, Caloiero *et al.* 2018, Ali *et al.* 2019). However, it is known that this test may be inaccurate in determining trends in the case of serial correlation (Kalra *et al.* 2017). Therefore, it is necessary to make an assumption of independence to ensure that this test gives correct results.

In recent years, many graphical methods without such assumptions have been proposed for trend analysis (Şen 2012, 2014, 2017, 2018, Güçlü 2018, Şen *et al.* 2019, Güçlü *et al.* 2020). In these methods, it is not important that the data do not fit the normal distribution, the length of data length can be short, and the data have a serial dependency (Şen 2012, 2017). In the innovative trend method (ITA) proposed by Şen (2012), the data can be divided into different groups such as low, medium, and high, and information can be obtained about important climatic events such as flood and drought. In the relevant study, this method was applied to the rainfall and flow data in various places in Turkey (Şen 2012). The results showed that in the case of trend presence, regardless of serial correlation or normal distribution, the data are located in the increasing or decreasing trend area in the Cartesian system. In addition, separating the data into low, medium, and high values provided information about the internal trend of the time series (Şen 2012). In contrast, only monotonic trends can be observed in Mann-Kendall test, and categorization is not possible. Also, while different trend situations can be seen with ITA (increasing/decreasing/no trend), it is impossible to see different trends with the Mann-Kendall test (Dabanlı *et al.* 2016).

In the innovative trend significance test (ITST) proposed by Şen (2017), the significance of the results obtained according to the innovative method proposed by Şen (2012) is tested by numerical calculations. The necessary statistical equations are supported by the linear trend slope method and the trend significance is tested. The method has been tested for different parameters at three points around the world (New Jersey – annual mean temperature, Danube River – annual mean flow, and Diyarbakır – annual total rainfall). Significant trends were observed at all stations (Şen 2017). The crossing trend method proposed by Şen (2018) aims to analyse trends based on the crossing characteristics of the time series. This method was applied with daily extreme rainfall in seven regions of Turkey, and the findings were compared with results of the Mann-Kendall test. The results of the two tests were not 100% compatible.

One of the novel methods in trend analysis is the innovative polygon trend analysis (IPTA) proposed by Şen *et al.* (2019). In this method, the trend of a time series can be determined, and information about the magnitude and slope of the trend transitions between consecutive segments (e.g. months) can be obtained. The one-year behaviour of time series can also be observed with this procedure. In this way, time-dependent internal variability can be evaluated. Şen *et al.* (2019) applied this procedure to monthly precipitation and flow data of selected stations in various parts of the world. The polygon templates were prepared in two ways: as arithmetic mean and as standard deviation. The results showed several increasing/decreasing trends over the months, and the slopes and lengths of these trends were calculated.

There are many studies using parametric and nonparametric methods in trend analysis of hydrometeorological data (Douglas *et al.* 2000, Cigizoglu *et al.* 2005, Partal and Kahya 2006, Zhang *et al.* 2008, Ceribasi *et al.* 2013, Silva *et al.* 2015, Gajbhiye *et al.* 2016, Diop *et al.* 2018, Meshram *et al.* 2020) In addition, graphical methods are used together with nonparametric methods such as Mann-Kendall test. The most frequently used graphical method in these studies is the ITA proposed by Şen (2012) (Haktanir and Citakoglu 2014, Saplıoğlu *et al.* 2014, Ay and Kisi 2015, Dabanlı *et al.* 2016, Wu and Qian 2017, Ahmad *et al.* 2018, Caloiero *et al.* 2018). Studies involving the ITST (Şen 2017) that test the significance of the proposed trend method have been increasing in recent years (Sanikhani *et al.* 2018, Ali *et al.* 2019, Ay 2020). The methods used in all these studies are summarized in Table 1.

Trend studies performed in Turkey have tended to focused on precipitation and temperature parameters (Partal and Kahya 2006, Dogan *et al.* 2015, Öztopal and Şen 2017, Hadi and Tombul 2018, Gumus 2019, Kankal and Akçay 2019b, Ay 2020, Sezen and Partal 2020). In addition, there are trend studies related to flows, although these are relatively few in number. These studies mainly cover the whole of Turkey and include stations belonging to the EBSB (Kahya and Kalayci 2004, Cigizoglu *et al.* 2005, Topaloğlu 2006, Yilmaz and Tosunoglu 2019). There are also a smaller number of studies conducted on the basin or regional scale. Kişi *et al.* (2018) evaluated trends in flow between the years 1967 and 2007 in three selected basins in Turkey. The EBSB is included in this study. Innovative trend, Mann-Kendall, and Sen's slope test were used to detect trends in their study. In a study conducted by Eris and Agiralioglu (2012) in the Eastern Black Sea Region, trend analysis was performed using the Mann-Kendall test with the data from 38 rainfall and 40 streamgauge stations covering a data range from 10 to 49 years. This regional study includes some stations in the EBSB. When past studies were examined, not a single study was found that included the last 10 years' worth of data and used graphic methods in the EBSB.

The aims of this study are as follows:

(a) To investigate the effects of land-use change and climate change on the monthly mean flows of stations located in the EBSB, a basin with significant water potential in Turkey, using long-term trend analysis;

Table 1. Previous studies.

| | Trend methods | | |
|---|---|---|---|
| Author(s) | Parametric methods | Nonparametric methods | Graphic methods |
| (Douglas *et al.* 2000) | | Mann-Kendall (regional average Kendall's S) | |
| (Cigizoglu *et al.* 2005) | t-test | Mann-Kendall | |
| (Partal and Kahya 2006) | | Sen's t-test<br>Mann-Kendall test<br>Sen's slope estimator | |
| (Zhang *et al.* 2008) | | Mann-Kendall test | |
| (Ceribasi *et al.* 2013) | | Mann-Kendall test<br>Spearman's rho test<br>Mann-Kendall rank correlation test | |
| (Saplıoğlu *et al.* 2014) | | Mann-Kendall | Innovative Şen's test |
| (Haktanir and Citakoglu 2014) | Linear regression test | Mann-Kendall test | Innovative Şen's test |
| (da Silva *et al.* 2015) | | Mann-Kendall<br>Sen's slope estimator | |
| (Ay and Kisi 2015) | | Mann-Kendall test | Innovative Şen's test |
| (Gajbhiye *et al.* 2016) | | Mann-Kendall test<br>Sen's slope estimator | |
| (Dabanlı *et al.* 2016) | | Mann-Kendall test | Innovative Şen's test |
| (Wu and Qian 2017) | Linear regression test | Mann-Kendall test | Innovative Şen's test |
| (Diop *et al.* 2018) | | Modified Mann-Kendall test<br>Sen's slope estimator | |
| (Ahmad *et al.* 2018) | | Mann-Kendall test<br>Sen's slope estimator | Innovative Şen's test |
| (Caloiero *et al.* 2018) | | Mann-Kendall test | Innovative Şen's test |
| (Sanikhani *et al.* 2018) | | Revised Mann-Kendall test<br>Sen's slope estimator | Innovative trend significance test |
| (Ali *et al.* 2019) | | Mann-Kendall test<br>Sen's slope estimator | Innovative trend significance test |
| (Ay 2020) | Linear regression test | Mann-Kendall test | Innovative trend significance test |
| (Meshram *et al.* 2020) | | Four Modified Mann-Kendall tests | |

(b) To observe the one-year behaviour of the stations by examining the transitions between months with the IPTA method, which will make it possible to determine the trends and slopes between the months;
(c) To make a seasonal assessment by taking into account the results of the months in the same season;
(d) To reveal the advantages and disadvantages of graphical methods by comparing innovative trend analysis methods (IPTA and ITST) and Mann-Kendall test.

In this context, first homogeneity analyses were performed on the data of 14 streamgauge stations from 1962–2018 (approximately 42 years) selected in the basin using absolute tests. Then, trend analyses of stations with homogeneous data were carried out. The application of the IPTA method is limited to flow data (Şen *et al.* 2019, Ahmed *et al.* 2021). In addition, it is the most comprehensive trend analysis study of river flows applied in the Eastern Black Sea Region, which is the region with the highest rainfall and the most flood events in Turkey.

## 2 Study area and data

The EBSB is situated on the northeast coast of Turkey. The basin is located between latitudes 40°15′ and 41°34′N and between longitudes 36°43′ and 41°35′E and is encompassed by the Eastern Black Sea Mountains to the south and the Black Sea to the north. The EBSB has the highest altitude and is the most mountainous part of the Black Sea Region. The basin's total area is 24.077 km$^2$, with an average surface water potential of 14.90 km$^3$ per year (Uzlu *et al.* 2011, Yüksek *et al.* 2013).

The EBSB receives an annual average rainfall of 1198 mm, making it the rainiest basin in Turkey (Odemis and Evrendilek 2007, Satılmış 2015). With the effect of topographic factors, precipitation rises from the east of Trabzon and becomes highest in Rize, Arhavi, and Hopa. Dominant wind direction, position, and elevation of slopes are the most important factors in the distribution of precipitation in the region (Karstarlı *et al.* 2011). The provinces' average yearly precipitation height values within the EBSB are 1045 mm for Ordu, 1288 mm for Giresun, 830 mm for Trabzon, 2304 mm for Rize, 693 mm for Artvin, 718 mm for Samsun, and 462 mm for Gümüşhane (GDM 2020). The basin has an average flow height of 753 mm per year. With this amount of flow, the share of the basin in the total flow of Turkey has been determined as 9.5%; with this feature, the EBSB has an important water potential (Odemis and Evrendilek 2007, Satılmış 2015).

Monthly data from 14 streamgauge stations located in the EBSB were used in this study (Fig. 1). Flow data were obtained from the General Directorate of State Hydraulic Works. Minimum and mean data lengths are 30 and 42 years, respectively. Data ranges vary but all fall between 1962 and 2018 (Table 2).

## 3 Methods

### 3.1 Homogeneity tests

Homogeneity tests can be used to reveal non-climatic changes in time series (Wijngaard *et al.* 2003). Absolute homogeneity tests were used in this study. A two-step method suggested by


**Figure 1.** Selected streamflow stations of the Eastern Black Sea basin.

**Table 2.** Station and record period of streamflow time series.

| Province | Station code | Station name | Altitude (m) | Record period | Record length (years) |
|---|---|---|---|---|---|
| Rize | D22A006 | Köprübaşı | 60 | 1967–2018 | 52 |
| | D22A062 | Konaklar | 300 | 1981–2010 | 30 |
| | D22A063 | Mikron Köprüsü | 325 | 1980–2013 | 34 |
| | E22A015 | Dereköy | 942 | 1987–2018 | 32 |
| | E22A032 | Topluca | 237 | 1965–2014 | 50 |
| | E22A033 | Tozköy | 1296 | 1967–2018 | 52 |
| Trabzon | D22A052 | Ulucami | 275 | 1980–2011 | 32 |
| | E22A002 | Ağnas | 78 | 1969–2018 | 50 |
| | E22A028 | Bahadırlı | 17 | 1962–2013 | 52 |
| | D22A007 | Şerah | 1114 | 1973–2018 | 46 |
| Giresun | D22A058 | Cücen Köprüsü | 300 | 1981–2012 | 32 |
| | E22A013 | Dereli | 248 | 1963–2004 | 42 |
| Ordu | E22A047 | Gocallı Köprüsü | 66 | 1969–2014 | 46 |
| Samsun | E22A045 | Gökçeli | 41 | 1970–2015 | 46 |

Wijngaard *et al.* (2003) was used to apply absolute methods. The first step is checking the homogeneity of stations using a standard normal homogeneity test (SNHT) (Alexandersson 1986), Pettitt test (Pettitt 1979), Buishand range (Buishand 1982), and von Neumann ratio (von Neumann 1941) were selected among absolute test types. For all these tests, homogeneity is checked by the null hypothesis ($H_0$): if $H_0$ is not rejected, the series is homogeneous and the data come from the same population. Otherwise, $H_0$ is rejected and there is a change. While SNHT, Pettitt and Buishand tests can detect the break year in the time series, this is not possible with the von Neumann test. In the second step, four tests were evaluated by classification. Three classes were use as follows:

- Class 1: Useful (if a maximum of one test out of four rejects $H_0$);
- Class 2: Doubtful (if two tests out of four reject $H_0$);
- Class 3: Suspect (if a minimum of three tests out of four reject $H_0$) (Wijngaard *et al.* 2003).

In this study, homogeneity analyses were performed with annual mean flow values (0.05 significance level). Stations that have doubtful data (Class 2) in terms of homogeneity were excluded from the study. Class 3 stations would be excluded also, but no stations fell into this category.

## 3.2 Trend analysis

### 3.2.1 Mann-Kendall test

In this method, the test statistic S is calculated as (Mann 1945, Kendall 1975):

$$S = \sum_{i=1}^{n-1} \sum_{j=i+1}^{n} sgn(x_j - x_i) \quad (1)$$

where n is the data length, and $x_i$ and $x_j$ indicate data values at times i and j, respectively.

$$sgn(x_j - x_i) = \begin{cases} 1; & x_j > x_i \\ 0; & x_j = x_i \\ -1; & x_j < x_i \end{cases} \quad (2)$$

When n > 10, the variance of S is calculated as:

$$Var(S) = \left[ n(n-1)(2n+5) - \sum_{i=1}^{p} t_i(t_i-1)(2t_i+5) \right] / 18 \quad (3)$$

In Equation (3), p is the number of tied groups. It means there is equal data in the time series. $t_i$ indicates how many times a datum repeats. Finally, the Z value is obtained from Equation (4):

$$Z = \begin{cases} \frac{S-1}{\sqrt{Var(S)}}, & S > 0 \\ 0, & 0 \\ \frac{S+1}{\sqrt{Var(S)}}, & S < 0 \end{cases} \quad (4)$$

As a result of this test, the existence of the trend is investigated with the null hypothesis. If the absolute value of the calculated Z value is greater than the standard z value corresponding to the chosen significance level (0.1, 0.05 or 0.01) the null hypothesis is

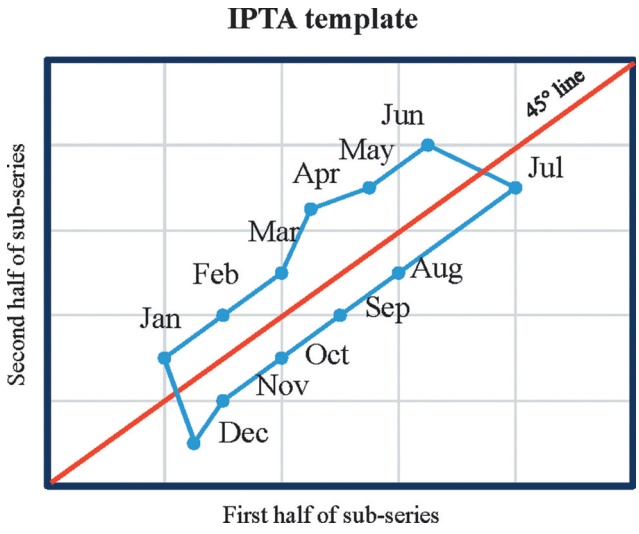


Figure 2. Innovative polygon trend analysis (IPTA) application (Şen *et al.* 2019).

rejected, in which case there is a trend. The sign of the S value determines the direction of the trend (positive means an increasing trend, negative means a decreasing trend). Otherwise, there is no trend in the time series and the null hypothesis is not rejected.

Before applying the Mann-Kendall test, it is essential to detect serial correlation with autocorrelation analysis (Yue *et al.* 2002). If a serial correlation is calculated significantly at the 95% confidence interval, it should be removed ($|r_1|>1{,}96/\sqrt{n}$) (Douglas *et al.* 2000). It can be eliminated with the trend-free pre-whitening method (TFPW) (Yue *et al.* 2002), which is widely used in the literature (Kumar *et al.* 2009, Meshram *et al.* 2020). In this study, before applying Mann-Kendall test, serial correlation is considered. In the overall analysis covering 132 months at 11 stations, serial dependency was determined in eight months and these dependencies were removed with TFPW.

### 3.2.2 Seasonal Kendall test

Using the seasonal Kendall test, Mann-Kendall test statistics for each season were calculated, and these are added for seasonal test statistics (Helsel *et al.* 2020):

$$S_k = \sum_{i=1}^{m} S_i \tag{5}$$

For this test, the season can be monthly or quarterly, or can follow any other time definition. In this study, monthly values were chosen as the season. The significance of the trend is investigated as in the classical Mann-Kendall test.

### 3.2.3 Innovative trend significance test

This trend method, proposed by Şen (2017), is based on the innovative trend method (Şen 2012). This method suggests a new statistical approach. First, time series are divided into two equal groups. The arithmetic average of each half series is calculated. The arithmetic average of the first series is $y_1$, the arithmetic average of the second series is $y_2$ and n is data length; the slope (s) of the trend is thus calculated as:

$$E(s) = \frac{2}{n}[E(\overline{y_2}) - E(\overline{y_1})] \tag{6}$$

$$\sigma_s^2 = \frac{8}{n^2}\left[E(\bar{y}_2^2) - E(\bar{y}_2\bar{y}_1)\right] \tag{7}$$

$$\rho_{\bar{y}_2\bar{y}_1} = \frac{E(\bar{y}_2\bar{y}_1) - E(\overline{y_2}) - E(\overline{y_1})}{\sigma_{\overline{y_2}}\sigma_{\overline{y_1}}} \tag{8}$$

$$\sigma_S^2 = \frac{8}{n^2}\frac{\sigma^2}{n}\left(1 - \rho_{\bar{y}_2\bar{y}_1}\right) \tag{9}$$

$$\sigma_S = \frac{2\sqrt{2}}{n\sqrt{n}}\sigma\sqrt{\left(1 - \rho_{\bar{y}_2\bar{y}_1}\right)} \tag{10}$$

Herein, E, ρ, $\sigma_s^2$ and $\sigma_s$ are expectations, the cross-correlation coefficient between two mean values, and the variance and standard deviation of the slope, respectively. Finally, the confidence limit of this test is obtained from Equation (11).

$$CL_{(1-\alpha)} = 0 \pm s_{cri}\sigma_s \tag{11}$$

where $s_{cri}$ represents critical z values at a designated significance level in the standard normal distribution. If the slope value is within the confidence intervals, there is no trend. Otherwise, there is a significant trend. In the case of s being positive (negative) there is an increasing (decreasing) trend.

### 3.2.4 Innovative polygon trend method

This trend procedure (Şen *et al.* 2019) is one of the innovative methods in the literature. In this method, the trend of a time series can be determined and knowledge about the magnitude and slope of trend transitions between consecutive segments (e.g. months) can be obtained. The method can be applied at different time scales such as daily, monthly, and yearly time series. In addition, when applying this method one can use the mean, minimum, maximum, standard deviation, and skewness parameters of time series.

For example, when analysing with monthly values, the method can be explained step by step as follows:

- First, all the time series (12 months) are divided into two equal groups.
- For each month, the mean (minimum, maximum, standard deviation, skewness, and so on) of the first and second half series is calculated.
- In the scatter diagram, the first half series is marked on the horizontal axis and the second is marked on the vertical axis. Moreover, the 12 scatter points are obtained.
- When successive points are connected with straight lines, a polygon is formed (Fig. 2).
- Finally, the slope and length of each straight line are calculated.

The length of the straight line between two points ($A(x_1,y_1)$; $B(x_2,y_2)$) can be calculated as:

$$|AB| = \sqrt{\left((x_2 - x_1)^2 + (y_2 - y_1)^2\right)} \tag{12}$$

and the slope of each straight line is obtained as:

$$s = \frac{y_2 - x_2}{y_1 - x_1} \quad (13)$$

In the Cartesian coordinate system 1:1 (45°), a straight line divides the diagram into two parts. If scatter points are above (below) the 1:1 line, there is an increasing (decreasing) trend (Şen 2012).

The straight lines connecting the points give information about the changes between months. If the slopes of the straight lines between the months are close to each other, the contribution of the changes between months to the average change in the time series is not significant. The polygon symbolizes the one-year behaviour of the time series. The more dynamic and complex a hydrometeorological event, the more complex the polygons that tend to arise (Şen *et al.* 2019).

## 4 Results

### 4.1 Homogeneity test results

The results of homogeneity tests are given in Table 3. In the table, inhomogeneous stations are marked in bold font. According to the test results, break years were determined

Table 3. Results of homogeneity tests for annual mean flows. (Bold expressions means inhomogeneous stations)

| Station Code | Test name | Test statistics | Result ($H_0$: rejected/not rejected) | Class |
|---|---|---|---|---|
| D22A006 | Pettitt | 153 | Not rejected | Class 1: Useful |
| | SNHT | 2.6337 | Not rejected | |
| | Buishand | 1.0712 | Not rejected | |
| | von Neumann | 1.8962 | Not rejected | |
| **D22A007** | **Pettitt** | **222** | **Rejected** | **Class 2: Doubtful** |
| | SNHT | 5.2967 | Not rejected | |
| | Buishand | 1.385 | Not rejected | |
| | **von Neumann** | **1.0404** | **Rejected** | |
| **D22A052** | Pettitt | 84 | Not rejected | **Class 2: Doubtful** |
| | SNHT | 3.1432 | Not rejected | |
| | **Buishand** | **1.6149** | **Rejected** | |
| | **von Neumann** | **1.3914** | **Rejected** | |
| D22A058 | Pettitt | 88 | Not rejected | Class 1: Useful |
| | SNHT | 4.0865 | Not rejected | |
| | Buishand | 1.7377 | Rejected | |
| | von Neumann | 1.5201 | Not rejected | |
| D22A062 | Pettitt | 111 | Rejected | Class 1: Useful |
| | SNHT | 5.9768 | Not rejected | |
| | Buishand | 1.0815 | Not rejected | |
| | von Neumann | 1.9204 | Not rejected | |
| D22A063 | Pettitt | 96 | Not rejected | Class 1: Useful |
| | SNHT | 2.4949 | Not rejected | |
| | Buishand | 1.2089 | Not rejected | |
| | von Neumann | 1.5635 | Not rejected | |
| E22A002 | Pettitt | 169 | Not rejected | Class 1: Useful |
| | SNHT | 2.9239 | Not rejected | |
| | Buishand | 1.1078 | Not rejected | |
| | von Neumann | 1.6243 | Not rejected | |
| E22A013 | Pettitt | 108 | Not rejected | Class 1: Useful |
| | SNHT | 3.7083 | Not rejected | |
| | Buishand | 0.85131 | Not rejected | |
| | von Neumann | 1.9202 | Not rejected | |
| E22A015 | Pettitt | 90 | Not rejected | Class 1: Useful |
| | SNHT | 3.7729 | Not rejected | |
| | Buishand | 1.4131 | Not rejected | |
| | von Neumann | 1.7954 | Not rejected | |
| E22A028 | Pettitt | 218 | Not rejected | Class 1: Useful |
| | SNHT | 5.8021 | Not rejected | |
| | Buishand | 1.1609 | Not rejected | |
| | von Neumann | 1.9261 | Not rejected | |
| **E22A032** | **Pettitt** | 275 | **Rejected** | **Class 2: Doubtful** |
| | **SNHT** | 10.53 | **Rejected** | |
| | Buishand | 1.4007 | Not rejected | |
| | von Neumann | 2.0918 | Not rejected | |
| E22A033 | Pettitt | 149 | Not rejected | Class 1: Useful |
| | SNHT | 2.3605 | Not rejected | |
| | Buishand | 1.1672 | Not rejected | |
| | von Neumann | 1.82 | Not rejected | |
| E22A045 | Pettitt | 157 | Not rejected | Class 1: Useful |
| | SNHT | 3.2727 | Not rejected | |
| | Buishand | 1.2083 | Not rejected | |
| | von Neumann | 2.0153 | Not rejected | |
| E22A047 | Pettitt | 192 | Not rejected | Class 1: Useful |
| | SNHT | 10.045 | Rejected | |
| | Buishand | 1.5256 | Not rejected | |
| | von Neumann | 1.5398 | Not rejected | |

for stations D22A007, D22A052, and E22A032 in 1998, 1993, and 2003, respectively. During these years, there may have been a change in the location of these stations or an error in the measurement method. Since D22A007, D22A052, and E22A032 were classified as doubtful, they were excluded from the study. Trend analysis was performed for the data from the remaining 11 stations.

## 4.2 Trend analysis results

### 4.2.1 Mann-Kendall test results

Mann-Kendall test results for 11 streamgauge stations are presented in Table 4. In this table, the months marked in bold show significant trends at the 95% confidence level.

According to the Mann-Kendall test results, most stations did not show significant trends in most months (0.05 significance level). For E22A033, the increasing trends in December, January, February, and March and the decreasing trends in July and August are noteworthy. Increasing trends were obtained for D22A062 in February, for D22A063 in October, and for E22A002 in March. For D22A006, an increasing trend in March and October and a decreasing trend in August was detected. A decreasing trend was observed in August for E22A047 and E22A015. Significant decreasing trends were detected in four of 11 stations in August.

### 4.2.2 Seasonal Kendall test results

Seasonal Kendall test results for 11 streamgauge stations are presented in Table 5. According to the seasonal Kendall test results, most stations did not show significant trends at a 0.05 significance level. Stations D22A062 and E22A033 showed increasing trends, while station E22A047 showed a decreasing trend. No significant trends were detected in the remaining stations.

### 4.2.3 ITST results

According to the ITST results, no trends were detected in 22 of the 132 months analysed. For the remaining months, an increasing trend was observed in 58 months and a decreasing trend in 52 months. The results of the innovative significance test at 95% confidence level are given in Table 6.

Using this method, radar charts showing slope, lower limit, and upper limit values are presented in Fig. 3 for stations D22A006, D22A058, D22A062, D22A063, E22A002, and E22A013 and in Fig 4 for stations E22A015, E22A028, E22A033, E22A045, and E22A047. There is no trend if the slope value is between the lower limit and the upper limit. However, if the slope value is above the upper limit, there is an increasing trend, and if the slope value is below the lower limit, there is a decreasing trend.

As shown in Fig. 3, the slope values are higher than the upper limit values in September–March, except in February at station D22A006, and there are increasing trends for these months. For the summer months (June, July, and August) the slope values are lower than the lower limit values, so decreasing trends were observed in these months. The rest of the months at this station did not show any trends. Also, there is a continuous increase in trend slope values from July to November.

For station D22A058, decreasing trends were observed in eight out of 12 months (January, March–August, and October). In addition to the spring and summer months, decreasing trends were observed in January and October, while increasing trends were observed in February and September.

At station D22A062, slope values are higher than the upper limit values, representing increasing trends in all autumn, winter, and spring months except April, which had no trend. As for the summer months, while there was an increasing trend in June, decreasing trends were observed in July and August. Also, there are continuously decreasing trend slope values from September to January.

There were decreasing trends in the summer months for station D22A063. Increasing trends were observed in September and October, in addition to the February–May period. While a decreasing trend was observed in January, no significant trends were detected in November and December.

At station E22A002, decreasing trends were observed in the April–November period, except for September, which had an increasing trend similar to January, February, and March. In December, a significant trend was not detected as the slope value was between the lower and upper limits.

Increasing trends were observed at station E22A013 in the October–February period. There was no trend in this station only in March. Significant decreasing trends were observed in the April–September period, except for June, which increased.

At station E22A015, an increasing trend was observed in February as well as in the spring months. Decreasing trends were detected in December, January, July, and August, with no trend in the remaining four months.

Significant increasing trends were observed at station E22A028 in September and November in addition to the February–July period. In August and December, decreasing trends were measured. There is a continuous increase in trend slope values for December–April.

Increasing trends were detected for the October–May period at station E22A033. Decreasing trends were observed in the summer months, and September was the only month that did not show any trend. Increasing trends were observed in almost all of the autumn, winter, and spring months. In addition to this, there is a continuous increase in trend slope values for January–May.

At station E22A045, decreasing trends were observed in the August–December period, while increasing trends were detected in the January–April period. No trend was observed in May, June, and July, as the slope values remained between the lower and upper limits.

At station E22A047, decreasing trends were detected in all months except January (increasing), September (increasing), and November (no trend). In addition, there are continuously decreasing trend slope values for January–May.

If a general assessment is made from the results obtained from this method, decreasing trends were largely observed in the monthly mean flows, especially during the summer months in the basin. The numbers of stations where we detected increasing, decreasing or no trend are presented in Table 7. The important point here is that there were significant decreasing trends at all 11 stations for August. For June and July, this

Table 4. Results of Mann-Kendall test for monthly mean flows (Bold expressions means significant trends)

| Station code | Months | Test statistic | Calculated Z value | Station code | Months | Test statistic | Calculated Z value | Station code | Months | Test statistic | Calculated Z value | Station code | Months | Test statistic | Calculated Z value |
|---|---|---|---|---|---|---|---|---|---|---|---|---|---|---|---|
| D22A006 | January | 149 | 1.1679 | D22A063 | January | 1 | 0.0000 | E22A015 | January | −65 | −1.0380 | E22A045 | January | 123 | 1.1552 |
| | February | 106 | 0.8287 | | February | 51 | 0.7412 | | February | 13 | 0.1946 | | February | 174 | 1.6384 |
| | **March** | 279 | **2.1938** | | March | 61 | 0.8895 | | March | 41 | 0.6487 | | March | 144 | 1.3540 |
| | April | 64 | 0.4972 | | April | 13 | 0.1779 | | April | −31 | −0.5099 | | April | −39 | −0.3598 |
| | May | 75 | 0.5841 | | May | 9 | 0.1186 | | May | 113 | 1.8170 | | May | −33 | −0.3030 |
| | June | −140 | −1.0971 | | June | 10 | 0.1334 | | June | −24 | −0.3730 | | June | 106 | 1.0271 |
| | July | −202 | −1.5862 | | July | −64 | −0.9345 | | July | −97 | −1.5570 | | July | 41 | 0.3787 |
| | **August** | −284 | **−2.2333** | | August | 11 | 0.1483 | | **August** | −137 | **−2.2057** | | August | −110 | −1.0321 |
| | September | 60 | 0.4656 | | September | 109 | 1.6010 | | September | −52 | −0.8270 | | September | −77 | −0.7196 |
| | **October** | 259 | **2.0360** | | October | 163 | **2.4016** | | October | −4 | −0.0486 | | October | −9 | −0.0758 |
| | November | 152 | 1.1916 | | November | 28 | 0.4003 | | November | −54 | −0.8597 | | November | 110 | 1.0321 |
| | December | 101 | 0.7891 | | December | 13 | 0.1779 | | December | −86 | −1.3784 | | December | −49 | −0.4545 |
| D22A058 | January | −42 | −0.6649 | E22A002 | January | 205 | 1.7064 | E22A028 | January | 127 | 0.9943 | E22A047 | January | 66 | 0.6156 |
| | February | 47 | 0.7461 | | February | 199 | 1.6562 | | February | −12 | −0.0868 | | February | 23 | 0.2083 |
| | March | 17 | 0.2595 | | **March** | 264 | **2.2005** | | March | 28 | 0.2131 | | March | −110 | −1.0322 |
| | April | −26 | −0.4057 | | April | 76 | 0.6275 | | April | 58 | 0.4498 | | April | −197 | −1.8559 |
| | May | −90 | −1.4433 | | May | −106 | −0.8784 | | May | −43 | −0.3314 | | May | −155 | −1.4582 |
| | June | −42 | −0.6649 | | June | −66 | −0.5438 | | June | 5 | 0.0316 | | June | −103 | −0.9659 |
| | July | −64 | −1.0216 | | July | −26 | −0.2091 | | July | −8 | −0.0552 | | July | −20 | −0.1799 |
| | August | −104 | −1.6707 | | August | −212 | −1.7650 | | August | −205 | −1.6098 | | **August** | −219 | **−2.0642** |
| | September | −10 | −0.1459 | | September | −47 | −0.3848 | | September | 56 | 0.4340 | | September | 2 | 0.0095 |
| | October | −35 | −0.5514 | | October | −73 | −0.6023 | | October | −127 | −0.9943 | | October | 20 | 0.1799 |
| | November | 5 | 0.0680 | | November | 9 | 0.0669 | | November | 71 | 0.5524 | | November | 103 | 0.9659 |
| | December | −52 | −0.8270 | | December | 3 | 0.0167 | | December | −135 | −1.0574 | | December | −139 | −1.3068 |
| D22A062 | January | 55 | 0.9634 | E22A013 | January | 65 | 0.6936 | E22A033 | **January** | 382 | **3.0077** | | | | |
| | **February** | 152 | **2.6944** | | February | 60 | 0.6394 | | **February** | 359 | **2.9078** | | | | |
| | March | 103 | 1.8204 | | March | −66 | −0.7046 | | **March** | 327 | **2.5727** | | | | |
| | April | 11 | 0.1784 | | April | 65 | 0.6937 | | April | 223 | 1.7521 | | | | |
| | May | 81 | 1.4273 | | May | −40 | −0.4380 | | May | 179 | 1.4048 | | | | |
| | June | 54 | 0.9942 | | June | 12 | 0.1236 | | June | −81 | −0.6314 | | | | |
| | July | −57 | −0.9994 | | July | −159 | −1.7125 | | **July** | −367 | **−2.8882** | | | | |
| | August | 9 | 0.1428 | | August | −154 | −1.6584 | | **August** | −362 | **−2.8490** | | | | |
| | September | 91 | 1.6057 | | September | −40 | −0.4227 | | September | −65 | −0.5051 | | | | |
| | October | 92 | 1.6238 | | October | 38 | 0.4010 | | October | 183 | 1.4362 | | | | |
| | November | 45 | 0.7850 | | November | 150 | 1.6149 | | November | 188 | 1.4759 | | | | |
| | December | 110 | 1.9450 | | December | 44 | 0.4660 | | **December** | 339 | **2.6676** | | | | |

Table 5. Results of seasonal Kendall test for monthly mean flows (95%).

| Station code | Slope | Calculated Z values | Trend |
|---|---|---|---|
| D22A006 | 0.01 | 1.41 | No significant trend |
| D22A058 | −0.02 | −1.71 | No significant trend |
| D22A062 | 0.09 | 3.90 | Increasing trend |
| D22A063 | 0.02 | 1.72 | No significant trend |
| E22A002 | 0.00 | 0.54 | No significant trend |
| E22A013 | 0.00 | 0.14 | No significant trend |
| E22A015 | −0.02 | −1.64 | No significant trend |
| E22A028 | 0.00 | −0.41 | No significant trend |
| E22A033 | 0.01 | 2.91 | Increasing trend |
| E22A045 | 0.01 | 1.16 | No significant trend |
| E22A047 | −0.05 | −1.99 | Decreasing trend |

number is 6 (55%) and 9 (82%), respectively. The stations showing increasing trends in autumn, winter and spring are higher than those showing decreasing trends. In February and March, the number of stations with an increasing trend is 9 (82%) and 8 (73%), respectively.

The province with the most stations within the scope of the study is Rize, with five stations: D22A006, D22A062, D22A063, E22A015, and E22A033. Here, significant increasing trends were observed in all five stations in March. Decreasing trends were determined at all five stations for July and August. In the other months, increasing trends were commonly measured.

#### 4.2.4 IPTA results

IPTA graphs are shown in Fig 5 for stations D22A006, D22A058, D22A062, and D22A063; in Fig. 6 for stations E22A002, E22A013, E22A015, and E22A028; and in Fig. 7 for stations E22A033, E22A045, and E22A047. In addition, trend volumes and slopes between consecutive months are presented for stations D22A006, D22A058, D22A062, D22A063, E22A002, and E22A013 in Table 8 and for stations E22A015, E22A028, E22A033, E22A045, and E22A047 in Table 9.

In the arithmetic mean graph of average flows for station D22A006, a distinct decreasing trend from the upward to downward trend area is seen in the transition from May (very close to the 1:1 line) to June. Only summer months are in the decreasing trend area, with strong downward trends far away from the 45° line. Again, there is a transition from decreasing to increasing area from August to September. Although the transition to the increase area lasts until the summer months, the amount (distance to the 1:1 line) is only high in autumn. In the standard deviation graph, while September showed a strong increasing trend, July, August, and October showed significant decreasing trends. The remaining months are usually scattered close to the 45° line. The inclusion of one month in the standard deviation graph in the increasing area indicates that the values in the second half differ more from the average than the values in the first half do. In other words, it shows that there are deteriorations in the flow regime during these months. The trend volumes range from 0.29 to 8.08 ($m^3$/s) for the mean, and trend slopes range from −15.24 to 9.27.

For station D22A058, there is a transition from January to February from the downward to the upward area in the arithmetic mean graph. Again, the transition from the upward to the downward trend area from February to March is a long trend, and the following five months are in this region. There is a serious decreasing tendency in the period of April–August. There is a sharp transition from August to September towards the upward trend area, and then there is a transition from September to October from the upward to the downward trend area. In the three months following October, the polygon ends in the downward trend area. A different polygon is seen on the standard deviation graph. All months showed strong trends except January. While March, May–August and October are in the decreasing area, the remaining months are in the increasing trend area. The trend volumes range from 0.57 to 6.80 ($m^3$/s) for the mean, and the slopes range from −1.42 to 7.15.

In the arithmetic mean graph, only July, August, and April are in the decreasing trend area at station D22A062. Transitions between March–April, April–May, and June–July are long, so the flows vary significantly between these months. December, January, and February are very close, so the changes between these months are very small. In the standard deviation graph, only July and August are in the downward trend area. There is a significant increasing trend, especially in May, in the months with increasing trends. The trend volumes range from 0.73 to 27.29 ($m^3$/s) for the mean, and trend slopes range from −8.27 to 2.45.

At station D22A063, the polygon starts with a transition from January to February from the downward to the upward trend area in the arithmetic mean graph. The three months following February are in an increasing area. There is a sharp transition from May to June from the upward to the downward trend area. While the summer months are in the decreasing region, the transition from August to September is from the downward to the upward area. The trends in September–October are larger than in other months in the increasing region as they are farther away from the 45° line. The transition from October to November is in the upward trend area but in a decreasing direction. The polygon ends almost immediately above the 45° line in December. There is a transition from the upward to the downward area from March to April and from May to June in the standard deviation graph. While the summer months and April are in the decreasing area, the remaining months are in the increasing trend area. The trend volumes and trend slope range from 0.52 to 14.98 ($m^3$/s) for the mean, whereas trend slopes range from −17.51 to 1.93.

Increasing trends are observed at station E22A002 from January to March in the arithmetic mean graph. There is a long transition from March to April from the increasing to the decreasing area. This means that there was a significant change between March and April. This change can be explained as follows: According to the values of the first half series, the values in April increased by three times compared to March. In the second half, the ratio decreased by approximately two times with the increase in March values and the decrease in April values. It is in the decreasing trend area in the four months following April. There is a transition from August to September towards the increasing trend area. September is very close to the 45° line, and the transition from September to October is towards the decreasing trend area. Although the transition from October to November is in a decreasing trend

**Table 6.** Results of innovative significance test for monthly mean flows (95%). (Bold expressions means significant trends)

| Station code | Months | Slope (s) | Lower limit | Upper limit | Trend | Station code | Months | Slope (s) | Lower limit | Upper limit | Trend |
|---|---|---|---|---|---|---|---|---|---|---|---|
| D22A006 | **January** | 0.0190 | −0.0047 | 0.0047 | + | E22A002 | January | 0.0191 | −0.0036 | 0.0036 | + |
| | February | 0.0018 | −0.0054 | 0.0054 | 0 | | **February** | 0.0291 | −0.0071 | 0.0071 | + |
| | **March** | 0.0168 | −0.0077 | 0.0077 | + | | **March** | 0.1083 | −0.0138 | 0.0138 | + |
| | April | 0.0055 | −0.0075 | 0.0075 | 0 | | **April** | −0.0558 | −0.0169 | 0.0169 | - |
| | May | 0.0034 | −0.0137 | 0.0137 | 0 | | **May** | −0.1520 | −0.0340 | 0.0340 | - |
| | **June** | −0.0520 | −0.0129 | 0.0129 | - | | **June** | −0.1445 | −0.0128 | 0.0128 | - |
| | **July** | −0.0835 | −0.0227 | 0.0227 | - | | **July** | −0.0131 | −0.0094 | 0.0094 | - |
| | **August** | −0.0529 | −0.0044 | 0.0044 | - | | **August** | −0.0324 | −0.0049 | 0.0049 | - |
| | **September** | 0.0448 | −0.0132 | 0.0132 | + | | **September** | 0.0099 | −0.0033 | 0.0033 | + |
| | **October** | 0.0503 | −0.0204 | 0.0204 | + | | **October** | −0.0335 | −0.0077 | 0.0077 | - |
| | **November** | 0.0518 | −0.0063 | 0.0063 | + | | **November** | −0.0121 | −0.0076 | 0.0076 | - |
| | **December** | 0.0118 | −0.0067 | 0.0067 | + | | December | 0.0018 | −0.0052 | 0.0052 | 0 |
| D22A058 | **January** | −0.0352 | −0.0087 | 0.0087 | - | E22A013 | **January** | 0.0224 | −0.0123 | 0.0123 | + |
| | **February** | 0.0412 | −0.0155 | 0.0155 | + | | **February** | 0.0302 | −0.0105 | 0.0105 | + |
| | **March** | −0.0511 | −0.0319 | 0.0319 | - | | March | −0.0346 | −0.0408 | 0.0408 | 0 |
| | **April** | −0.0225 | −0.0172 | 0.0172 | - | | **April** | −0.1104 | −0.0950 | 0.0950 | - |
| | **May** | −0.1609 | −0.0324 | 0.0324 | - | | **May** | −0.0231 | −0.0211 | 0.0211 | - |
| | **June** | −0.1090 | −0.0192 | 0.0192 | - | | **June** | 0.0556 | −0.0328 | 0.0328 | + |
| | **July** | −0.0853 | −0.0249 | 0.0249 | - | | **July** | −0.0589 | −0.0095 | 0.0095 | - |
| | **August** | −0.0893 | −0.0206 | 0.0206 | - | | **August** | −0.0573 | −0.0167 | 0.0167 | - |
| | **September** | 0.0340 | −0.0223 | 0.0223 | + | | **September** | −0.0339 | −0.0106 | 0.0106 | - |
| | **October** | −0.0482 | −0.0165 | 0.0165 | - | | **October** | 0.0742 | −0.0116 | 0.0116 | + |
| | November | −0.0132 | −0.0294 | 0.0294 | 0 | | **November** | 0.1405 | −0.0179 | 0.0179 | + |
| | December | −0.0220 | −0.0272 | 0.0272 | 0 | | **December** | 0.0197 | −0.0192 | 0.0192 | + |
| D22A062 | **January** | 0.0443 | −0.0099 | 0.0099 | + | E22A015 | **January** | −0.0168 | −0.0058 | 0.0058 | - |
| | **February** | 0.1084 | −0.0305 | 0.0305 | + | | **February** | 0.0233 | −0.0085 | 0.0085 | + |
| | **March** | 0.0624 | −0.0416 | 0.0416 | + | | **March** | 0.1352 | −0.0313 | 0.0313 | + |
| | April | −0.0343 | −0.0884 | 0.0884 | 0 | | **April** | 0.0459 | −0.0273 | 0.0273 | + |
| | **May** | 0.2834 | −0.0934 | 0.0934 | + | | **May** | 0.3886 | −0.0406 | 0.0406 | + |
| | **June** | 0.0770 | −0.0622 | 0.0622 | + | | June | 0.0102 | −0.0830 | 0.0830 | 0 |
| | **July** | −0.3087 | −0.0443 | 0.0443 | - | | **July** | −0.1800 | −0.0501 | 0.0501 | - |
| | **August** | −0.0535 | −0.0193 | 0.0193 | - | | **August** | −0.0901 | −0.0211 | 0.0211 | - |
| | **September** | 0.2026 | −0.0344 | 0.0344 | + | | September | −0.0011 | −0.0104 | 0.0104 | 0 |
| | **October** | 0.1172 | −0.0342 | 0.0342 | + | | October | −0.0125 | −0.0265 | 0.0265 | 0 |
| | **November** | 0.0923 | −0.0336 | 0.0336 | + | | November | −0.0125 | −0.0265 | 0.0265 | 0 |
| | **December** | 0.0518 | −0.0092 | 0.0092 | + | | **December** | −0.0254 | −0.0093 | 0.0093 | - |
| D22A063 | **January** | −0.0184 | −0.0058 | 0.0058 | - | E22A028 | January | 0.0001 | −0.0049 | 0.0049 | 0 |
| | **February** | 0.0212 | −0.0080 | 0.0080 | + | | **February** | 0.0092 | −0.0039 | 0.0039 | + |
| | **March** | 0.0188 | −0.0176 | 0.0176 | + | | **March** | 0.0397 | −0.0076 | 0.0076 | + |
| | **April** | 0.0362 | −0.0271 | 0.0271 | + | | **April** | 0.0622 | −0.0058 | 0.0058 | + |
| | **May** | 0.0484 | −0.0284 | 0.0284 | + | | **May** | 0.0064 | −0.0036 | 0.0036 | + |
| | **June** | −0.0992 | −0.0489 | 0.0489 | - | | **June** | 0.0229 | −0.0061 | 0.0061 | + |
| | **July** | −0.1559 | −0.0196 | 0.0196 | - | | **July** | 0.0115 | −0.0034 | 0.0034 | + |
| | **August** | −0.0585 | −0.0183 | 0.0183 | - | | **August** | −0.0206 | −0.0043 | 0.0043 | - |
| | **September** | 0.1317 | −0.0287 | 0.0287 | + | | **September** | 0.0177 | −0.0026 | 0.0026 | + |
| | **October** | 0.1241 | −0.0184 | 0.0184 | + | | October | −0.0082 | −0.0125 | 0.0125 | 0 |
| | November | 0.0191 | −0.0206 | 0.0206 | 0 | | **November** | 0.0154 | −0.0056 | 0.0056 | + |
| | December | 0.0010 | −0.0156 | 0.0156 | 0 | | **December** | −0.0095 | −0.0051 | 0.0051 | - |
| E22A033 | **January** | 0.0108 | −0.0013 | 0.0013 | + | E22A047 | January | −0.0175 | −0.0519 | 0.0519 | 0 |
| | **February** | 0.0145 | −0.0014 | 0.0014 | + | | **February** | −0.0878 | −0.0461 | 0.0461 | - |
| | **March** | 0.0312 | −0.0029 | 0.0029 | + | | **March** | −0.2540 | −0.0768 | 0.0768 | - |
| | **April** | 0.0650 | −0.0129 | 0.0129 | + | | **April** | −0.4945 | −0.1176 | 0.1176 | - |
| | **May** | 0.0987 | −0.0102 | 0.0102 | + | | **May** | −0.5792 | −0.0815 | 0.0815 | - |
| | **June** | −0.0490 | −0.0137 | 0.0137 | - | | **June** | −0.2620 | −0.0807 | 0.0807 | - |
| | **July** | −0.1008 | −0.0048 | 0.0048 | - | | **July** | −0.0255 | −0.0153 | 0.0153 | - |
| | **August** | −0.0285 | −0.0027 | 0.0027 | - | | **August** | −0.0405 | −0.0148 | 0.0148 | - |
| | September | 0.0007 | −0.0011 | 0.0011 | 0 | | **September** | 0.0208 | −0.0110 | 0.0110 | + |
| | **October** | 0.0247 | −0.0027 | 0.0027 | + | | **October** | −0.0826 | −0.0348 | 0.0348 | - |
| | **November** | 0.0213 | −0.0031 | 0.0031 | + | | November | −0.0044 | −0.0316 | 0.0316 | 0 |
| | **December** | 0.0174 | −0.0012 | 0.0012 | + | | **December** | −0.2040 | −0.0380 | 0.0380 | - |
| E22A045 | **January** | 0.0319 | −0.0072 | 0.0072 | + | | | | | | |
| | **February** | 0.0606 | −0.0092 | 0.0092 | + | | | | | | |
| | **March** | 0.0345 | −0.0302 | 0.0302 | + | | | | | | |
| | **April** | 0.0261 | −0.0130 | 0.0130 | + | | | | | | |
| | May | −0.0201 | −0.0237 | 0.0237 | 0 | | | | | | |
| | June | 0.0054 | −0.0170 | 0.0170 | 0 | | | | | | |
| | July | −0.0112 | −0.0205 | 0.0205 | 0 | | | | | | |
| | **August** | −0.0756 | −0.0204 | 0.0204 | - | | | | | | |
| | **September** | −0.0134 | −0.0089 | 0.0089 | - | | | | | | |
| | **October** | −0.0713 | −0.0232 | 0.0232 | - | | | | | | |
| | **November** | −0.0281 | −0.0194 | 0.0194 | - | | | | | | |
| | **December** | −0.0312 | −0.0104 | 0.0104 | - | | | | | | |

(0): No trend (+): Increasing trend (-): Decreasing trend

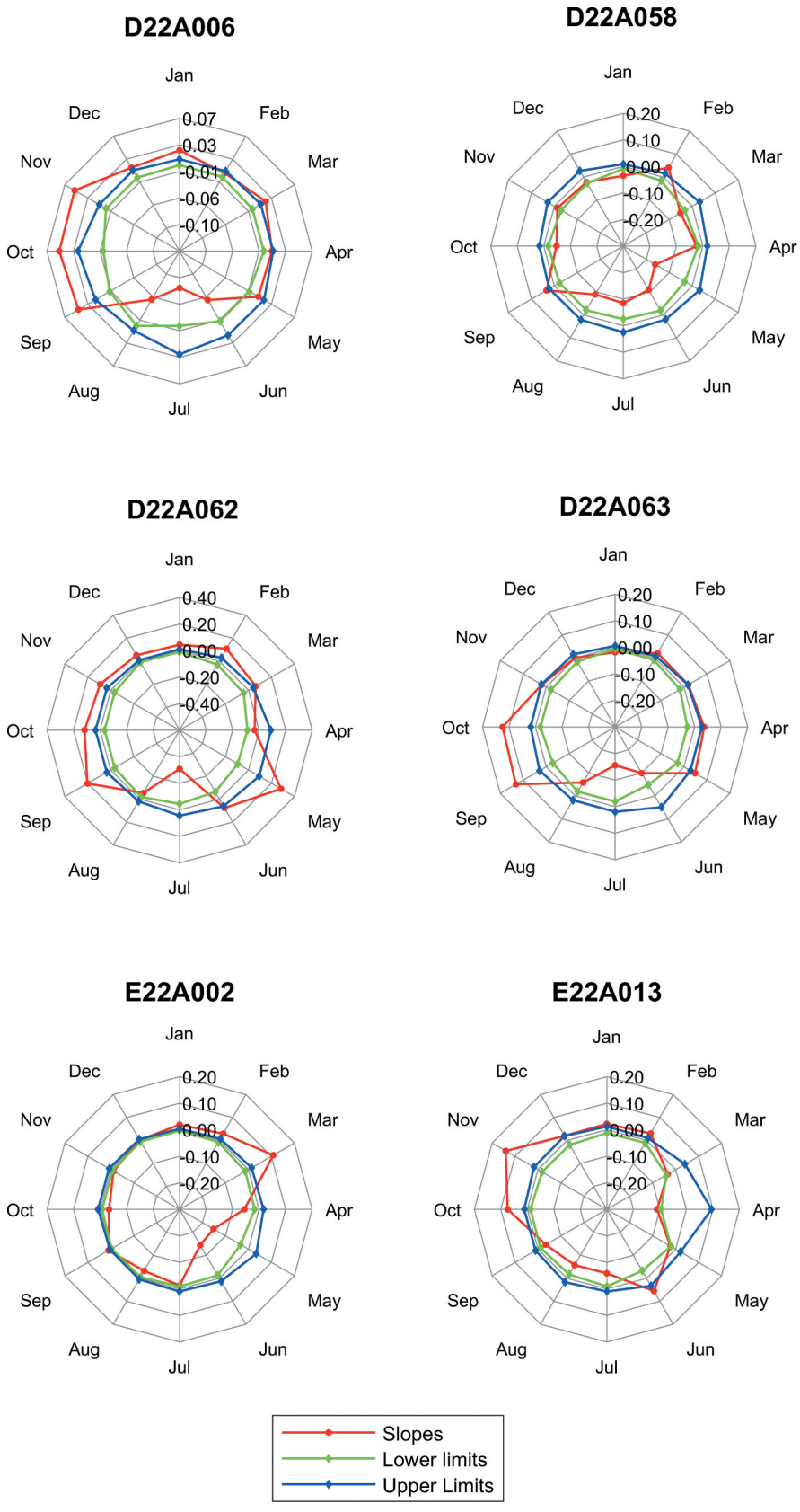


**Figure 3.** Innovative trend significance test radar charts for stations D22A006, D22A058, D22A062, D22A063, E22A002, and E22A013.

area, it is in an increasing direction. December is above the 45° line. Flow values do not vary much between December, January, and February. In the standard deviation graph, the January–May period is in the increasing area. Transitions from May to June and from July to August are from the upward to the downward area. March, May, and June showed strong trends. The trend volumes range from 0.75 to 24.20 ($m^3/s$) for the mean, and the trend slopes range from −3.38 to 10.75.

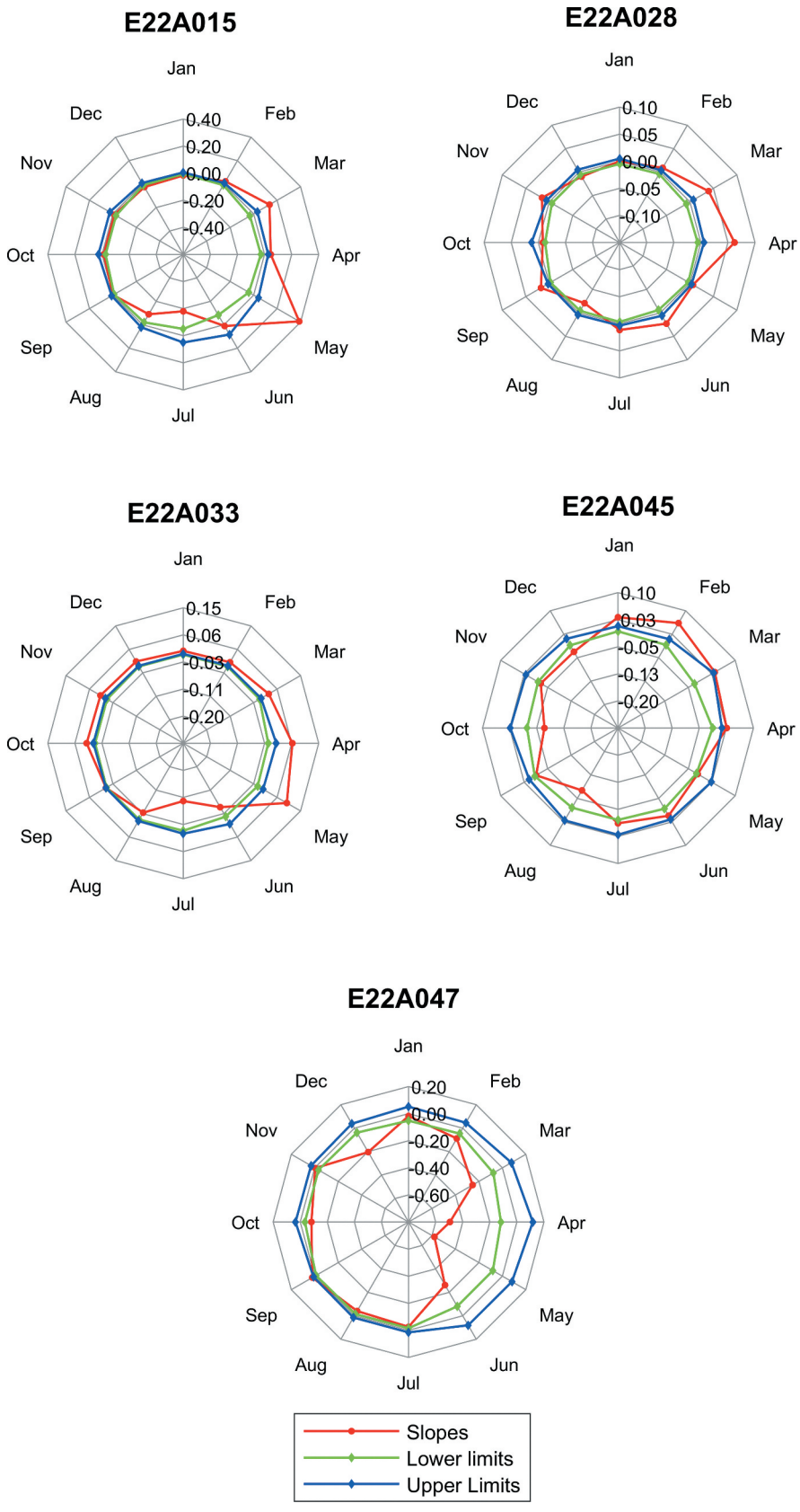


**Figure 4.** Innovative trend significance test radar charts for stations E22A015, E22A028, E22A033, E22A045, and E22A047.

Since most of the months are close to the 45° line at station E22A013, a narrow polygon is formed on the arithmetic mean graph. This situation caused the trends to be similar and produced a low slope between months. February–March and June–July transitions are from the increasing to the decreasing area. August and September are also in the decreasing area. There is a transition from September to October from the decreasing to the increasing area. The two months following

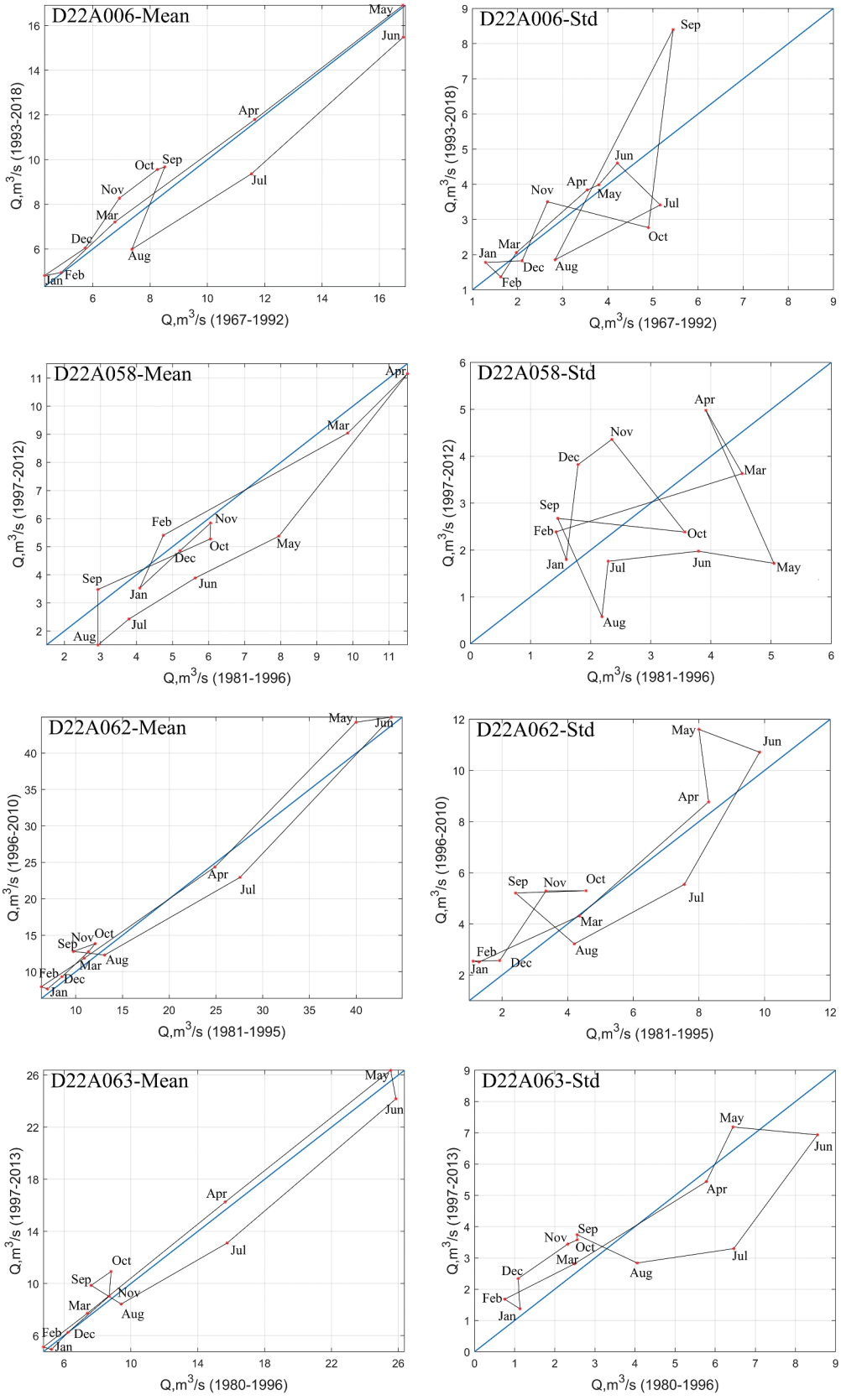


**Figure 5.** Innovative polygon trend analysis graphs for stations D22A006, D22A058, D22A062, and D22A063.

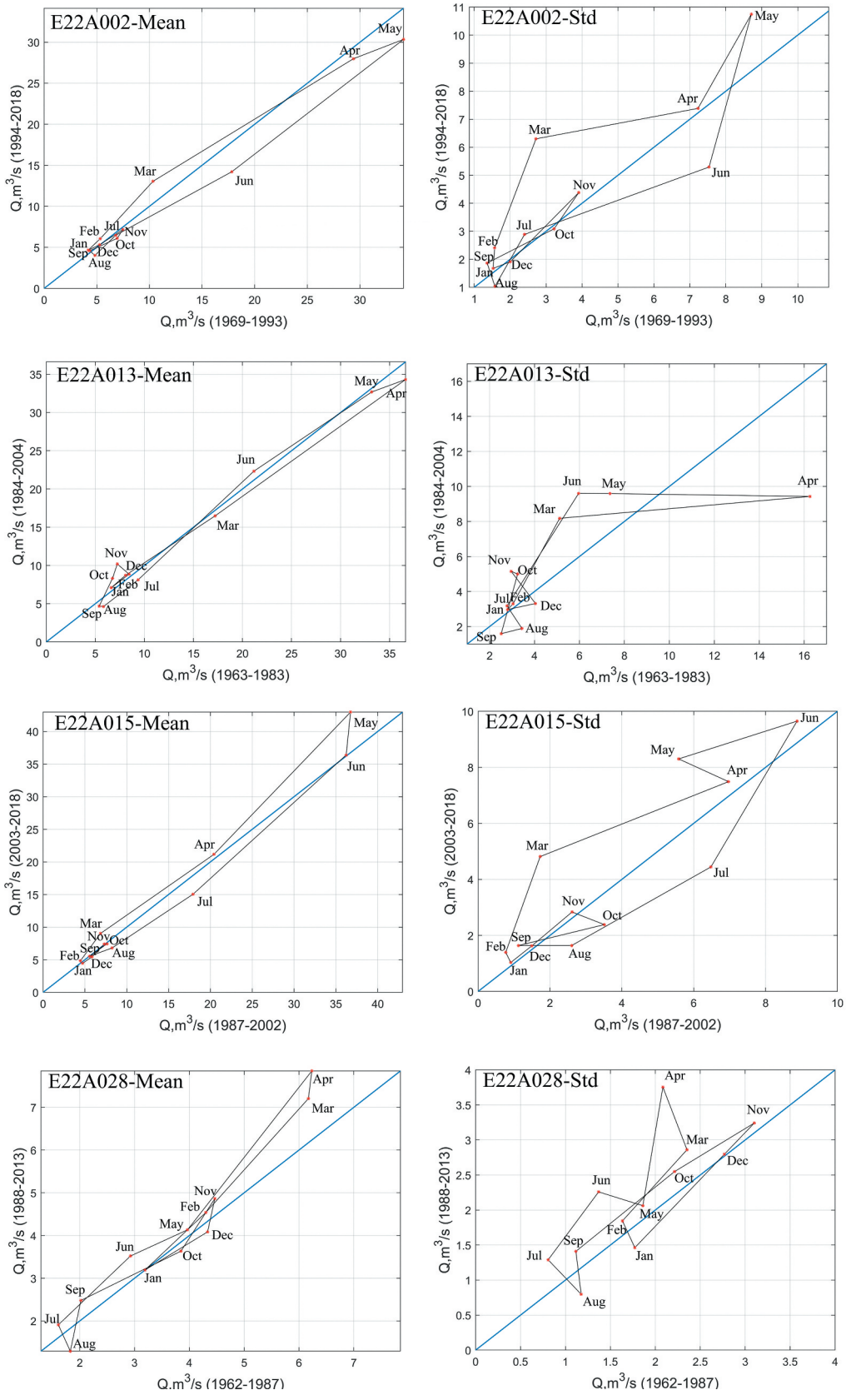


**Figure 6.** Innovative polygon trend analysis graphs for stations E22A002, E22A013, E22A015, and E22A028.

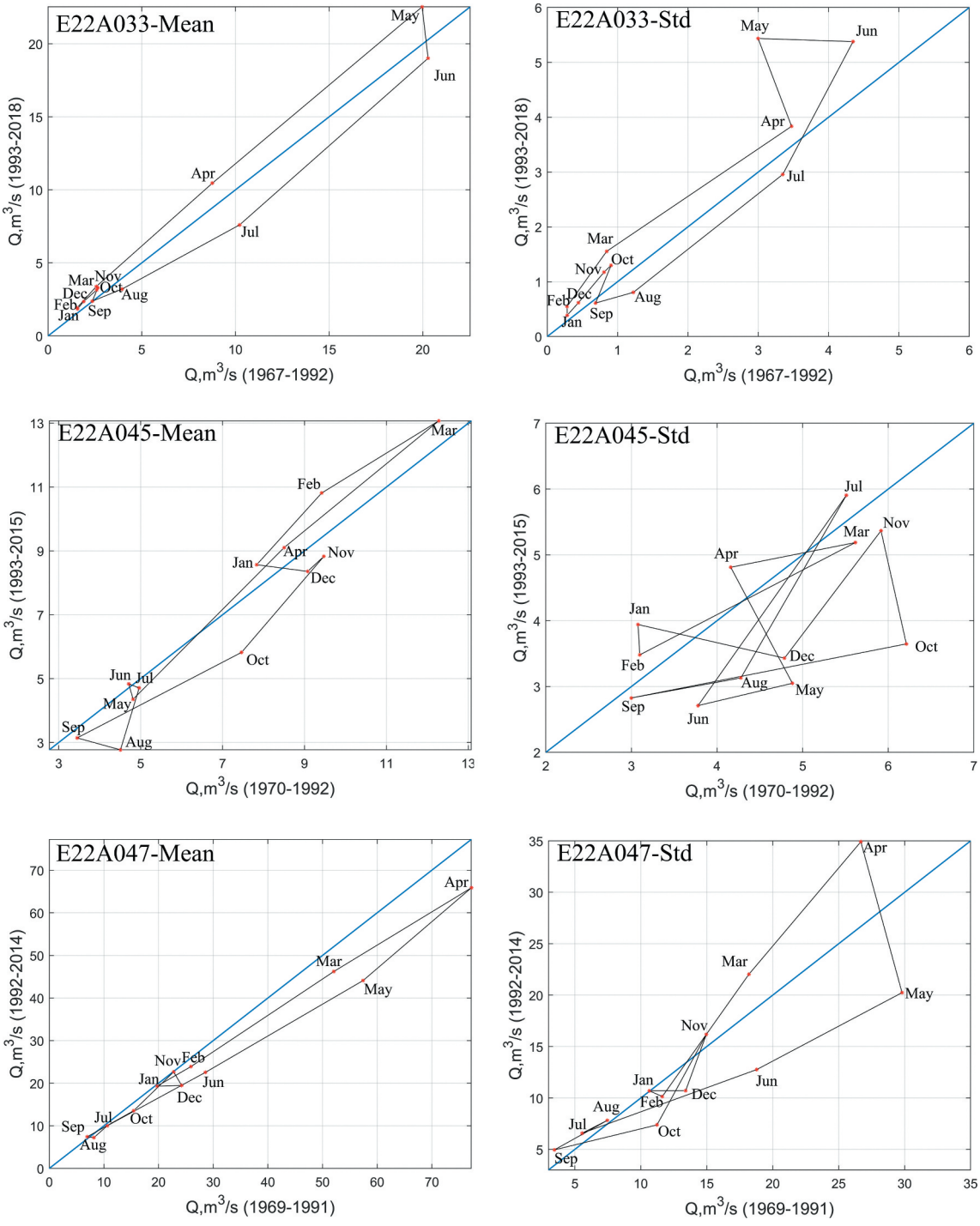


**Figure 7.** Innovative polygon trend analysis graphs for stations E22A033, E22A045, and E22A047.

October are in the increasing trend area. December, January, and February are scattered close to each other and the changes in these months are small. April is remarkable in the standard deviation graph. The transition of March–April is from the upward to the downward area. The transition from April to May is towards the increasing area again. In addition to April showing a significant decreasing trend, September, August, and December are also in the decreasing trend area. The trend volumes range from 0.44 to 26.37 ($m^3/s$) for the mean, and here, trend slopes range from −2.41 to 3.19.

At station E22A015, since January and February are very close to the 45° line, a trend is not seen in the arithmetic mean graph. The spring months following February are in the region of increasing trend. There is a significant decreasing trend in the transition from May to June. June is above the 45° line, so there is no trend in this month. The months of July and August are in the decreasing region. September, October, and November are scattered very close to the 45° line. December is located in the decreasing area. In the standard deviation graph, the period January–June is in the increasing area.

Table 7. Number of stations with detected trends (increasing/decreasing/no trend).

| | Number of stations (total 11) | | |
|---|---|---|---|
| Months | Increasing trend | Decreasing trend | No trend |
| January | 6 | 3 | 2 |
| February | 9 | 1 | 1 |
| March | 8 | 2 | 1 |
| April | 5 | 4 | 2 |
| May | 5 | 4 | 2 |
| June | 3 | 6 | 2 |
| July | 1 | 9 | 1 |
| August | 0 | 11 | 0 |
| September | 7 | 2 | 2 |
| October | 5 | 4 | 2 |
| November | 5 | 2 | 4 |
| December | 4 | 4 | 3 |

Transitions from June to July and from September to October are from the upward to the downward areas. With the transition from October to November, the polygon ended in the increasing area with December. The trend volumes range from 0.34 to 28.12 ($m^3/s$) for the mean, and the trend slopes range from −17.61 to 11.67.

Only August, October, and December are in the decreasing trend area at station E22A028. The remaining months except January showed increasing trends in the arithmetic mean graph. The increasing trends in the spring months are remarkable. There is an important transition from July to August, from the increasing area to the decreasing area. In the standard deviation graph, only January and August are in the decreasing area. April showed a strong increasing trend. The trend volumes range from 0.65 to 4.36 ($m^3/s$) for the mean while the trend slopes range from −1.88 to 105.76. The maximum slope is due to the change from January to February. This large slope occurs because the means of the first and second half series are very close to each other in January in the arithmetic mean. Thus, a large slope value was obtained due to the small difference between January values in the denominator in the slope calculation.

At station E22A033, the polygon started with January in the increasing area, and increasing trends continued until May in the arithmetic mean graph. It can be seen that the flows changed significantly during the transitions from March to April and from April to May. The May–June transition is sharp from the increasing area to the decreasing area. In the summer months, decreasing trends are observed. September is above the 45° line and there is no trend for this month. The transition from September to October is towards the increasing trend area. In addition, the two months following October are in the increasing trend area. The standard deviation and the mean plots show a single polygon and an almost general direction. This means it maintained a natural equilibrium state for a year. Furthermore, only July, August, and September are in the decreasing trend area. May and June showed strong increasing trends, where the trend volumes range from 0.07 to 16.47 ($m^3/s$) for the mean and trend slopes range from −0.50 to 35.51.

Flows at station E22A045 show a different polygon with more than one loop. There is a transition from the downward area to the upward area from December to January in the arithmetic mean graph. The three months following January are in the increasing trend area. From April to May, there is a long transition from the upward area to the downward area. June is almost above the 45° line. The transition from June to July is towards the decreasing trend area. The July–December period is in the decreasing trend area. In the autumn months, strong decreasing trends are observed. The standard deviation graph shows a complex polygon with multiple loops. While January, February, April, and July are in the increasing area, the remaining months are in the decreasing trend area. The trend volumes range from 0.28 to 6.01 ($m^3/s$) for the mean, whereas the trend slopes range from −2.05 to 6.78.

In the arithmetic mean graph, significant decreasing trends, especially in the spring months, draw attention at station E22A047. The months of January, November, September, and July are quite close to the 45° line, so it is concluded that there is no trend for these months. Transitions from February to March and from May to June are quite long, so flows change significantly between these months. There is no month in the increasing trend area. A different polygon is seen on the standard deviation graph. Strong increases in April and decreasing trends in May are noteworthy. The trend volumes range from 1.23 to 36 ($m^3/s$) for the mean, and the trend slopes range from −3.98 to 46.31.

According to the results obtained by this method, similar to the ITST results, decreasing trends were observed in the monthly mean flows especially during the summer months in the basin. There are decreasing trends at all stations in August. Decreasing trends were observed in July at all stations to the east of the basin. While there is a decreasing trend at most stations in June, an increasing trend was observed in three stations located in the middle and eastern parts. Except for station E22A033, we observed more than one large–small pooling in the mean and standard deviation graphs and not in a single direction. For this reason, there is no natural equilibrium, no homogeneous and isotropic state in flows.

### 4.3 Comparison of trend methods and general assessment

The results of all methods except seasonal Kendall test are shown in Table 10. While there are significant trends in 14 of 132 months according to the Mann-Kendall method, these results overlap with the results of the other two innovative methods. ITST and IPTA results are highly (90%) consistent with each other. The decreasing trends in the summer months are remarkable throughout the basin. Again, according to the results obtained from innovative trend approaches, increasing trends in the east of the basin in the autumn and spring months are apparent. In the stations located in the middle part of the basin, decreasing trends were determined in the spring and summer months except for one station. At station E22A045 situated in the far west of the basin, the decreasing trend that started in the summer months continued until the end of the year. Decreasing trends in most months at station E22A047, in the western part of the basin, also draw attention.

Seasonal Kendall test could not be added to Table 10 because it considers all months together and gives a holistic result. According to the seasonal Kendall test results,

**Table 8.** Innovative polygon trend analysis monthly statistical values for stations D22A006, D22A058, D22A062, D22A063, E22A002 and E22A013.

| | | Months | | | | | | | | | | | |
|---|---|---|---|---|---|---|---|---|---|---|---|---|---|
| | | January | February | March | April | May | June | July | August | September | October | November | December |
| | D22A006 | | | | | | | | | | | | |
| Mean | 1st half ($m^3/s$) | 4.32 | 4.90 | 6.77 | 11.65 | 16.82 | 16.83 | 11.54 | 7.37 | 8.51 | 8.25 | 6.93 | 5.73 |
| | 2nd half ($m^3/s$) | 4.81 | 4.95 | 7.21 | 11.80 | 16.91 | 15.48 | 9.37 | 5.99 | 9.68 | 9.56 | 8.28 | 6.04 |
| SD | 1st half ($m^3/s$) | 1.29 | 1.63 | 1.97 | 3.54 | 3.80 | 4.21 | 5.16 | 2.83 | 5.45 | 4.90 | 2.66 | 2.10 |
| | 2nd half ($m^3/s$) | 1.78 | 1.37 | 2.06 | 3.84 | 3.99 | 4.60 | 3.41 | 1.86 | 8.40 | 2.77 | 3.50 | 1.82 |
| | | Jan–Feb | Feb–Mar | Mar–Apr | Apr–May | May–Jun | Jun–Jul | Jul–Aug | Aug–Sep | Sep–Oct | Oct–Nov | Nov–Dec | Dec–Jan |
| Mean | Trend volume ($m^3/s$) | 0.60 | 2.94 | 6.70 | 7.27 | 1.43 | 8.08 | 5.37 | 3.86 | 0.29 | 1.83 | 2.54 | 1.88 |
| | Trend slope | 0.10 | 9.27 | 0.33 | 0.62 | −15.24 | 1.60 | 0.63 | −0.85 | 1.12 | 1.03 | 0.23 | 1.61 |
| SD | Trend volume ($m^3/s$) | 0.53 | 0.77 | 2.37 | 0.30 | 0.74 | 1.52 | 2.80 | 7.05 | 5.66 | 2.35 | 1.77 | 0.81 |
| | Trend slope | −0.54 | −0.32 | 3.51 | 0.62 | 2.14 | −4.45 | 0.56 | −3.02 | −0.72 | −0.39 | −0.33 | −1.77 |
| | D22A058 | | | | | | | | | | | | |
| Mean | 1st half ($m^3/s$) | 4.09 | 4.75 | 9.86 | 11.52 | 7.95 | 5.63 | 3.79 | 2.94 | 2.93 | 6.05 | 6.06 | 5.21 |
| | 2nd half ($m^3/s$) | 3.53 | 5.41 | 9.04 | 11.16 | 5.38 | 3.89 | 2.43 | 1.51 | 3.48 | 5.28 | 5.85 | 4.86 |
| SD | 1st half ($m^3/s$) | 1.60 | 1.43 | 4.52 | 3.92 | 5.05 | 3.79 | 2.29 | 2.19 | 1.45 | 3.57 | 2.35 | 1.79 |
| | 2nd half ($m^3/s$) | 1.80 | 2.39 | 3.63 | 4.98 | 1.72 | 1.98 | 1.76 | 0.58 | 2.68 | 2.38 | 4.36 | 3.82 |
| | | Jan–Feb | Feb–Mar | Mar–Apr | Apr–May | May–Jun | Jun–Jul | Jul–Aug | Aug–Sep | Sep–Oct | Oct–Nov | Nov–Dec | Dec–Jan |
| Mean | Trend volume ($m^3/s$) | 1.99 | 6.28 | 2.69 | 6.80 | 2.75 | 2.35 | 1.25 | 1.97 | 3.60 | 0.57 | 1.30 | 1.74 |
| | Trend slope | −1.17 | −1.24 | 0.44 | 7.15 | 0.68 | 0.78 | 1.05 | −0.38 | −1.42 | 0.27 | 1.67 | 1.60 |
| SD | Trend volume ($m^3/s$) | 0.62 | 3.33 | 1.48 | 3.45 | 1.28 | 1.51 | 1.19 | 2.22 | 2.13 | 2.32 | 0.78 | 2.03 |
| | Trend slope | 4.80 | −0.92 | −1.20 | −3.13 | 0.55 | 0.29 | 3.03 | −0.76 | −0.97 | −1.70 | 1.01 | 0.10 |
| | D22A062 | | | | | | | | | | | | |
| Mean | 1st half ($m^3/s$) | 6.98 | 6.32 | 10.92 | 24.89 | 39.98 | 43.77 | 27.59 | 13.10 | 9.75 | 12.09 | 11.37 | 8.54 |
| | 2nd half ($m^3/s$) | 7.65 | 7.94 | 11.86 | 24.38 | 44.23 | 44.93 | 22.96 | 12.30 | 12.79 | 13.85 | 12.75 | 9.31 |
| SD | 1st half ($m^3/s$) | 1.12 | 1.30 | 4.36 | 8.30 | 8.00 | 9.85 | 7.55 | 4.20 | 2.41 | 4.56 | 3.34 | 1.93 |
| | 2nd half ($m^3/s$) | 2.55 | 2.51 | 4.31 | 8.77 | 11.61 | 10.71 | 5.55 | 3.22 | 5.21 | 5.30 | 5.29 | 2.57 |
| | | Jan–Feb | Feb–Mar | Mar–Apr | Apr–May | May–Jun | Jun–Jul | Jul–Aug | Aug–Sep | Sep–Oct | Oct–Nov | Nov–Dec | Dec–Jan |
| Mean | Trend volume ($m^3/s$) | 0.73 | 6.04 | 18.77 | 24.93 | 3.86 | 27.29 | 17.99 | 3.39 | 2.58 | 1.32 | 4.45 | 2.28 |
| | Trend slope | 2.45 | 0.58 | −0.55 | −8.27 | 0.27 | −4.01 | 0.17 | −3.79 | 0.58 | 0.79 | 0.56 | 0.86 |
| SD | Trend volume ($m^3/s$) | 0.18 | 3.55 | 5.95 | 2.85 | 2.06 | 5.65 | 4.08 | 2.67 | 2.15 | 1.22 | 3.06 | 0.81 |
| | Trend slope | 0.85 | −0.04 | −9.82 | 7.55 | 0.24 | −2.32 | 0.49 | −2.85 | 0.26 | 2.64 | 0.33 | 2.22 |
| | D22A063 | | | | | | | | | | | | |
| Mean | 1st half ($m^3/s$) | 5.25 | 4.76 | 7.40 | 15.65 | 25.54 | 25.86 | 15.77 | 9.42 | 7.62 | 8.81 | 8.70 | 6.23 |
| | 2nd half ($m^3/s$) | 4.94 | 5.12 | 7.71 | 16.26 | 26.37 | 24.18 | 13.11 | 8.42 | 9.86 | 10.92 | 9.03 | 6.25 |
| SD | 1st half ($m^3/s$) | 1.13 | 0.75 | 2.49 | 5.78 | 6.44 | 8.55 | 6.46 | 4.05 | 2.56 | 2.56 | 2.32 | 1.09 |
| | 2nd half ($m^3/s$) | 1.37 | 1.68 | 2.81 | 5.44 | 7.19 | 6.94 | 3.30 | 2.84 | 3.74 | 3.58 | 3.44 | 2.34 |
| | | Jan–Feb | Feb–Mar | Mar–Apr | Apr–May | May–Jun | Jun–Jul | Jul–Aug | Aug–Sep | Sep–Oct | Oct–Nov | Nov–Dec | Dec–Jan |
| Mean | Trend volume ($m^3/s$) | 0.52 | 3.69 | 11.88 | 14.15 | 2.21 | 14.98 | 7.89 | 2.30 | 1.60 | 1.90 | 3.72 | 1.63 |
| | Trend slope | −1.16 | 0.88 | 1.93 | 1.34 | −2.05 | 1.57 | 0.38 | −2.25 | 0.94 | 0.15 | 0.05 | −17.51 |
| SD | Trend volume ($m^3/s$) | 0.49 | 2.07 | 4.21 | 1.87 | 2.12 | 4.19 | 2.45 | 1.75 | 0.16 | 0.28 | 1.65 | 0.97 |
| | Trend slope | 3.86 | 0.34 | −1.06 | −2.20 | −2.17 | 1.96 | 0.38 | −0.98 | 0.86 | 1.10 | 1.12 | 0.19 |
| | E22A002 | | | | | | | | | | | | |
| Mean | 1st half ($m^3/s$) | 4.18 | 5.33 | 10.34 | 29.38 | 34.15 | 17.83 | 6.81 | 4.83 | 4.33 | 6.95 | 7.49 | 5.27 |
| | 2nd half ($m^3/s$) | 4.66 | 6.06 | 13.05 | 27.99 | 30.35 | 14.21 | 6.48 | 4.02 | 4.58 | 6.11 | 7.18 | 5.31 |
| SD | 1st half ($m^3/s$) | 1.53 | 1.57 | 2.72 | 7.22 | 8.71 | 7.53 | 2.40 | 1.58 | 1.36 | 3.22 | 3.91 | 2.00 |
| | 2nd half ($m^3/s$) | 1.68 | 2.41 | 6.30 | 7.39 | 10.75 | 5.29 | 2.89 | 1.04 | 1.87 | 3.09 | 4.38 | 1.91 |
| | | Jan–Feb | Feb–Mar | Mar–Apr | Apr–May | May–Jun | Jun–Jul | Jul–Aug | Aug–Sep | Sep–Oct | Oct–Nov | Nov–Dec | Dec–Jan |
| Mean | Trend volume ($m^3/s$) | 1.81 | 8.60 | 24.20 | 5.32 | 22.95 | 13.47 | 3.16 | 0.75 | 3.03 | 1.20 | 2.90 | 1.27 |
| | Trend slope | 1.53 | 3.72 | −0.52 | 2.72 | 0.95 | 0.09 | 2.48 | −0.31 | −3.38 | 0.36 | −0.15 | 10.75 |

(*Continued*)

**Table 8.** (Continued).

| | | | | | | | | | | | | | |
|---|---|---|---|---|---|---|---|---|---|---|---|---|---|
| SD | Trend volume ($m^3/s$) | 0.73 | 4.06 | 4.63 | 3.67 | 5.58 | 5.67 | 2.03 | 0.86 | 2.23 | 1.46 | 3.12 | 0.53 |
| | Trend slope | 5.65 | 4.27 | 0.04 | 12.65 | −1.10 | −0.22 | −1.11 | −0.94 | −0.27 | −3.52 | −0.19 | −1.65 |
| | E22A013 | | | | | | | | | | | | |
| Mean | 1st half ($m^3/s$) | 6.63 | 8.08 | 17.22 | 36.64 | 33.17 | 21.17 | 9.36 | 5.83 | 5.39 | 6.75 | 7.24 | 8.45 |
| | 2nd half ($m^3/s$) | 7.10 | 8.71 | 16.49 | 34.32 | 32.69 | 22.33 | 8.12 | 4.63 | 4.68 | 8.31 | 10.19 | 8.86 |
| SD | 1st half ($m^3/s$) | 2.80 | 3.04 | 5.12 | 16.26 | 7.36 | 5.96 | 2.78 | 3.44 | 2.52 | 3.25 | 2.96 | 4.04 |
| | 2nd half ($m^3/s$) | 2.97 | 3.30 | 8.18 | 9.43 | 9.59 | 9.60 | 3.18 | 1.89 | 1.59 | 5.00 | 5.15 | 3.32 |
| | | Jan–Feb | Feb–Mar | Mar–Apr | Apr–May | May–Jun | Jun–Jul | Jul–Aug | Aug–Sep | Sep–Oct | Oct–Nov | Nov–Dec | Dec–Jan |
| Mean | Trend volume ($m^3/s$) | 2.17 | 12.00 | 26.37 | 3.84 | 15.85 | 18.48 | 4.96 | 0.44 | 3.88 | 1.94 | 1.80 | 2.53 |
| | Trend slope | 1.35 | −1.14 | 3.19 | 0.21 | −2.41 | −1.06 | 0.97 | 0.59 | −2.19 | 1.89 | 0.14 | 1.14 |
| SD | Trend volume ($m^3/s$) | 0.41 | 5.30 | 11.21 | 8.90 | 1.40 | 7.17 | 1.44 | 0.97 | 3.48 | 0.33 | 2.13 | 1.29 |
| | Trend slope | 1.52 | 11.88 | −2.23 | −0.33 | 1.63 | 0.11 | −3.90 | 0.60 | −1.89 | 1.25 | −0.33 | −0.24 |

SD: standard deviation.

**Table 9.** Innovative polygon trend analysis monthly statistical values for stations E22A015, E22A028, E22A033, E22A045 and E22A047.

| | | Months | | | | | | | | | | | |
|---|---|---|---|---|---|---|---|---|---|---|---|---|---|
| | | January | February | March | April | May | June | July | August | September | October | November | December |
| | E22A015 | | | | | | | | | | | | |
| Mean | 1st half ($m^3/s$) | 4.72 | 4.46 | 6.86 | 20.42 | 36.75 | 36.22 | 17.92 | 8.24 | 5.55 | 7.64 | 7.30 | 5.84 |
| | 2nd half ($m^3/s$) | 4.45 | 4.83 | 9.03 | 21.16 | 42.96 | 36.39 | 15.04 | 6.80 | 5.53 | 7.44 | 7.40 | 5.44 |
| SD | 1st half ($m^3/s$) | 0.91 | 0.77 | 1.73 | 6.97 | 5.58 | 8.88 | 6.48 | 2.60 | 1.12 | 3.51 | 2.61 | 1.49 |
| | 2nd half ($m^3/s$) | 1.03 | 1.40 | 4.81 | 7.49 | 8.30 | 9.65 | 4.44 | 1.64 | 1.64 | 2.38 | 2.84 | 1.63 |
| | | Jan–Feb | Feb–Mar | Mar–Apr | Apr–May | May–Jun | Jun–Jul | Jul–Aug | Aug–Sep | Sep–Oct | Oct–Nov | Nov–Dec | Dec–Jan |
| Mean | Trend volume ($m^3/s$) | 0.46 | 4.84 | 18.20 | 27.24 | 6.60 | 28.12 | 12.71 | 2.98 | 2.83 | 0.34 | 2.45 | 1.50 |
| | Trend slope | −1.39 | 5.80 | 0.34 | 8.46 | 0.03 | −17.61 | 0.50 | 0.01 | 11.67 | −0.47 | −4.32 | 0.66 |
| SD | Trend volume ($m^3/s$) | 0.39 | 3.55 | 5.88 | 1.61 | 3.56 | 5.73 | 4.78 | 1.48 | 2.50 | 1.00 | 1.65 | 0.84 |
| | Trend slope | 5.06 | 4.92 | 0.17 | 5.23 | 0.28 | −2.63 | 0.47 | −0.53 | −2.19 | −0.20 | 0.60 | 0.94 |
| | E22A028 | | | | | | | | | | | | |
| Mean | 1st half ($m^3/s$) | 3.19 | 4.30 | 6.17 | 6.23 | 3.97 | 2.93 | 1.61 | 1.83 | 2.02 | 3.85 | 4.47 | 4.33 |
| | 2nd half ($m^3/s$) | 3.19 | 4.54 | 7.21 | 7.85 | 4.13 | 3.52 | 1.91 | 1.29 | 2.48 | 3.63 | 4.87 | 4.09 |
| SD | 1st half ($m^3/s$) | 1.77 | 1.63 | 2.35 | 2.08 | 1.86 | 1.37 | 0.81 | 1.17 | 1.12 | 2.21 | 3.10 | 2.77 |
| | 2nd half ($m^3/s$) | 1.46 | 1.84 | 2.86 | 3.75 | 2.06 | 2.26 | 1.29 | 0.80 | 1.41 | 2.55 | 3.24 | 2.80 |
| | | Jan–Feb | Feb–Mar | Mar–Apr | Apr–May | May–Jun | Jun–Jul | Jul–Aug | Aug–Sep | Sep–Oct | Oct–Nov | Nov–Dec | Dec–Jan |
| Mean | Trend volume ($m^3/s$) | 1.74 | 3.26 | 0.65 | 4.36 | 1.21 | 2.08 | 0.65 | 1.20 | 2.16 | 1.38 | 0.79 | 1.45 |
| | Trend slope | 105.76 | 4.33 | 1.57 | 0.10 | 3.56 | 0.50 | −1.79 | −0.86 | −0.46 | −1.88 | −0.62 | −0.01 |
| SD | Trend volume ($m^3/s$) | 0.41 | 1.24 | 0.93 | 1.71 | 0.53 | 1.12 | 0.61 | 0.62 | 1.58 | 1.13 | 0.56 | 1.67 |
| | Trend slope | −0.68 | 2.41 | 3.29 | 0.12 | 4.44 | 0.54 | −0.78 | −0.78 | 1.14 | 0.42 | 0.20 | −11.09 |
| | E22A033 | | | | | | | | | | | | |
| Mean | 1st half ($m^3/s$) | 1.58 | 1.55 | 2.58 | 8.77 | 19.97 | 20.28 | 10.23 | 3.95 | 2.36 | 2.66 | 2.60 | 1.90 |
| | 2nd half ($m^3/s$) | 1.86 | 1.93 | 3.39 | 10.46 | 22.53 | 19.01 | 7.61 | 3.21 | 2.38 | 3.31 | 3.15 | 2.36 |
| SD | 1st half ($m^3/s$) | 0.28 | 0.28 | 0.85 | 3.47 | 3.00 | 4.35 | 3.35 | 1.22 | 0.69 | 0.91 | 0.81 | 0.44 |
| | 2nd half ($m^3/s$) | 0.39 | 0.55 | 1.55 | 3.83 | 5.44 | 5.38 | 2.96 | 0.81 | 0.61 | 1.30 | 1.17 | 0.62 |
| | | Jan–Feb | Feb–Mar | Mar–Apr | Apr–May | May–Jun | Jun–Jul | Jul–Aug | Aug–Sep | Sep–Oct | Oct–Nov | Nov–Dec | Dec–Jan |
| Mean | Trend volume ($m^3/s$) | 0.07 | 1.79 | 9.39 | 16.47 | 3.53 | 15.21 | 7.67 | 1.78 | 0.97 | 0.17 | 1.05 | 0.60 |
| | Trend slope | 1.34 | 2.16 | 2.08 | 1.52 | −0.50 | 2.06 | 0.28 | −0.02 | 35.51 | 0.86 | 0.82 | 0.62 |
| SD | Trend volume ($m^3/s$) | 0.16 | 1.15 | 3.48 | 1.67 | 1.35 | 2.62 | 3.02 | 0.57 | 0.72 | 0.16 | 0.67 | 0.28 |
| | Trend slope | 2.56 | 2.66 | 0.51 | 6.77 | 0.42 | −0.38 | 1.07 | 0.18 | −5.13 | 0.94 | 0.47 | 0.60 |
| | E22A045 | | | | | | | | | | | | |
| Mean | 1st half ($m^3/s$) | 7.83 | 9.42 | 12.28 | 8.50 | 4.82 | 4.71 | 4.96 | 4.51 | 3.45 | 7.46 | 9.47 | 9.08 |
| | 2nd half ($m^3/s$) | 8.57 | 10.81 | 13.07 | 9.10 | 4.36 | 4.84 | 4.71 | 2.77 | 3.14 | 5.82 | 8.83 | 8.36 |
| SD | 1st half ($m^3/s$) | 3.08 | 3.10 | 5.62 | 4.16 | 4.88 | 3.78 | 5.51 | 4.28 | 3.00 | 6.21 | 5.92 | 4.79 |
| | 2nd half ($m^3/s$) | 3.94 | 3.48 | 5.19 | 4.81 | 3.05 | 2.71 | 5.91 | 3.13 | 2.83 | 3.65 | 5.37 | 3.43 |
| | | Jan–Feb | Feb–Mar | Mar–Apr | Apr–May | May–Jun | Jun–Jul | Jul–Aug | Aug–Sep | Sep–Oct | Oct–Nov | Nov–Dec | Dec–Jan |
| Mean | Trend volume ($m^3/s$) | 2.75 | 3.65 | 5.48 | 6.01 | 0.49 | 0.28 | 1.99 | 1.12 | 4.82 | 3.61 | 0.62 | 1.26 |
| | Trend slope | 1.90 | 0.57 | 0.76 | −0.77 | −0.27 | −2.05 | 6.78 | 0.18 | 5.34 | 0.39 | 1.11 | −1.02 |
| SD | Trend volume ($m^3/s$) | 0.46 | 3.04 | 1.50 | 1.90 | 1.15 | 3.64 | 3.04 | 1.32 | 3.32 | 1.74 | 2.24 | 1.78 |
| | Trend slope | 0.44 | −1.12 | −1.52 | −2.81 | 0.58 | −0.37 | −2.90 | 0.15 | 14.89 | 0.21 | 2.47 | −0.64 |
| | E22A047 | | | | | | | | | | | | |
| Mean | 1st half ($m^3/s$) | 19.70 | 25.93 | 52.06 | 77.24 | 57.42 | 28.58 | 10.60 | 8.16 | 6.95 | 15.44 | 22.76 | 24.20 |
| | 2nd half ($m^3/s$) | 19.30 | 23.91 | 46.22 | 65.87 | 44.10 | 22.55 | 10.01 | 7.23 | 7.42 | 13.54 | 22.66 | 19.51 |

(*Continued*)

Table 9. (Continued).

| | | | | | | | | | | | | | |
|---|---|---|---|---|---|---|---|---|---|---|---|---|---|
| SD | 1st half ($m^3/s$) | 10.65 | 11.63 | 18.20 | 26.68 | 29.80 | 18.79 | 5.55 | 7.47 | 3.45 | 11.23 | 14.97 | 13.40 |
| | 2nd half ($m^3/s$) | 10.70 | 10.14 | 22.04 | 34.92 | 20.24 | 12.77 | 6.58 | 7.83 | 4.96 | 7.38 | 16.18 | 10.72 |
| | | Jan–Feb | Feb–Mar | Mar–Apr | Apr–May | May–Jun | Jun–Jul | Jul–Aug | Aug–Sep | Sep–Oct | Oct–Nov | Nov–Dec | Dec–Jan |
| Mean | Trend volume ($m^3/s$) | 7.74 | 34.36 | 31.94 | 29.45 | 36.00 | 21.92 | 3.70 | 1.23 | 10.47 | 11.69 | 3.46 | 4.50 |
| | Trend slope | 5.02 | 2.89 | 1.95 | 1.17 | 0.45 | 0.10 | 1.59 | −0.51 | −3.98 | 0.05 | 46.31 | 0.09 |
| SD | Trend volume ($m^3/s$) | 1.13 | 13.59 | 15.42 | 15.00 | 13.31 | 14.62 | 2.29 | 4.94 | 8.15 | 9.56 | 5.69 | 2.75 |
| | Trend slope | −28.40 | −2.58 | 2.15 | −1.16 | 0.63 | −0.17 | 0.35 | 4.18 | −2.56 | −0.32 | −2.21 | −0.02 |

SD: standard deviation.

Table 10. Comparison of trend tests for monthly mean flows.

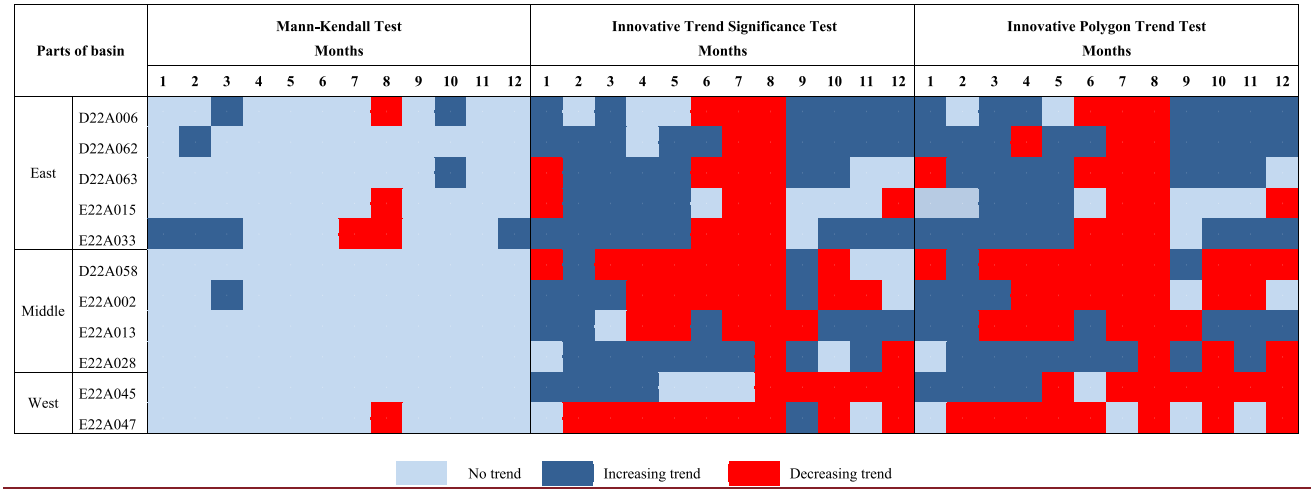


significant trends were detected only at three stations. According to the Mann-Kendall test, a trend was detected only in February at station D22A062 (increasing), while an increasing trend was detected according to the seasonal Kendall test. Again for station E22A047, a decreasing trend was seen in the seasonal Kendall test, while a significant trend was detected only in August with the Mann-Kendall test (decreasing). Finally, while the seasonal Mann-Kendall test determined an increasing trend at station E22A033, according to the Mann-Kendall test increasing trends were seen in December, January, February, and March; on the other hand, decreasing trends were detected in July and August. No significant trends were found in the other months.

## 5 Discussion

When previous studies were examined, no studies were found in which basin flows were analysed by applying innovative methods with many stations. Kişi *et al.* (2018) investigated the trend of the monthly mean data of nine streamgauge stations selected from three basins in Turkey between 1964 and 2007. Stations E22A018, E22A032, and E22A033 in the EBSB are included. In that study, in which Mann-Kendall and ITA methods were applied, both methods detected increasing trends at station E22A033, which agrees with our study. In this study, increasing trends were observed at station E22A033, except for the summer months, especially according to the innovative methods. According to the Mann-Kendall test, an increasing trend was detected in only four months. It is natural to observe differences in the results due to the different measurement intervals analysed. In addition, there are various studies in which several stations from the basin are included with statistical methods, even if they are not specific to the basin. Kahya and Kalayci (2004) investigated trends of 31-year monthly mean flows for 83 stations in Turkey using nonparametric Spearman's rho, Şen's t, Mann-Kendall, and seasonal Kendall methods, and they found no trends in the EBSB flows. Topaloğlu (2006) evaluated trends in monthly mean flows obtained from 84 streamgauge stations in Turkey between 1968 and 1997. According to the Mann-Kendall test, commonly statistically significant trends (95%) were not detected in the monthly flows of the EBSB. In our study, there were no substantial statistical trends in the Mann-Kendall test results. However, the detection of significant trends in multiple months compared to other methods reveals the sensitivity of the innovative methods. Again, in this study, finding a few trends by comparing previous studies to the Mann-Kendall test shows a change in trends over the years.

When the analysis of hydrometeorological data in the literature with innovative methods is examined, it can been seen that innovative methods such as those explored in this study are more sensitive in trend detection when compared to parametric methods such as Mann-Kendall. Alifujiang *et al.* (2021)

Table 11. Results of trend tests for total monthly rainfall.

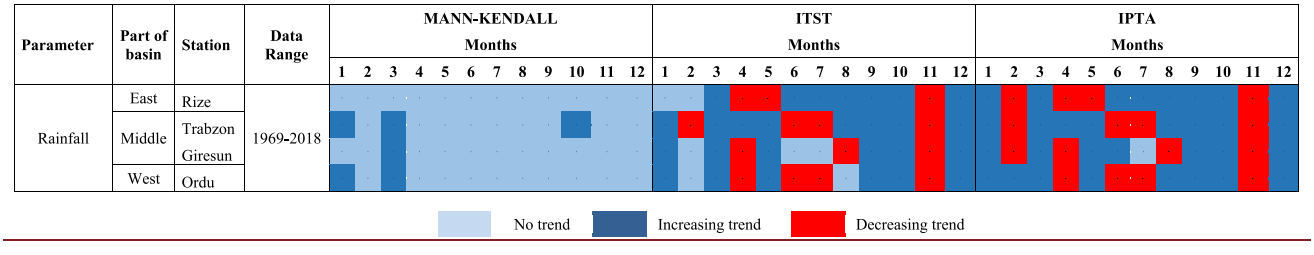

**Table 12.** Results of trend tests for monthly mean temperature.

| Parameter | Part of basin | Station | Data Range | MANN-KENDALL Months 1 2 3 4 5 6 7 8 9 10 11 12 | ITST Months 1 2 3 4 5 6 7 8 9 10 11 12 | IPTA Months 1 2 3 4 5 6 7 8 9 10 11 12 |
|---|---|---|---|---|---|---|
| Temperature | East | Rize | 1969-2018 | | | |
| | Middle | Trabzon | | | | |
| | | Giresun | | | | |
| | West | Ordu | | | | |

No trend  Increasing trend  Decreasing trend

performed a trend analysis of annual and seasonal mean flows in the Lake Issyk-Kul basin in Central Asia. ITST and Mann-Kendall test were used, and they found that ITST effectively revealed the trends determined by the Mann-Kendall test. Also, ITST found trends in more series than the Mann-Kendall test did. Şan *et al.* (2021) examined the trend of monthly total precipitation at 15 selected stations in Vu Gia–Thu Bon River basin in Vietnam. Mann-Kendall, ITST, and IPTA methods were used. The trend finding percentages in the analysed months were 26%, 93%, and 88% for Mann-Kendall, ITST, and IPTA, respectively; thus, it was observed that the percentage of trend detection is higher for the innovative methods than for the Mann-Kendall test for precipitation data. Similarly, the innovative methods were more sensitive in trend detection than the Mann-Kendall test for flow data in the present study. When the results of two different parameters in two different studies are taken into account, it is seen that the effectiveness of innovative methods is higher than that of classical methods, even if the studied parameter changes. Also, the polygons created for both parameters are multi-loop and chaotic since both are complex events.

In hydro-environmental systems, temperature and precipitation are the most effective meteorological variables (Nourani *et al.* 2019). As average temperatures at the Earth's surface rise, more evaporation occurs, which in turn increases the overall precipitation (EPA 2011). To examine the impact of climate change on flows in the region, trend analysis of precipitation and temperature values at four stations in the region was carried out for the years 1969–2018 (see Table 11 for rainfall and Table 12 for temperature). Mann-Kendall test, ITST, and IPTA methods were used for these analyses. There is an increasing trend in temperatures throughout the region. This increasing trend generally caused an increase in precipitation, except in April, the summer months, and November. The decrease in flow data in the summer months was caused by the decrease in both precipitation and effective evaporation in these months. In the eastern part, there was a decrease in precipitation in April, May and November, while there was an increase in flow data. This difference occurred because the flow stations in the eastern part are in the high mountainous regions, while the precipitation and temperatures are measured at the station near the sea. While there were decreases in precipitation in the western part only in April, June, July and November, there were decreases in flow data throughout the year, except for the first four months at station E22A045. This situation is thought to be caused by temperature increases and land use.

To reveal the relationship between flow values and land-use status in the EBSB, the per province land-use changes between 1990 and 2012 are presented in Table 13. In addition, the table shows the difference between 1990 and 2018 for the Melet River, Ordu, one of the most important basins in the EBSB. It was observed that there was an overall increase in residential area between 1990 and 2012, smaller from west to east. In the same period, an increase in industrial areas (<500 ha) and a decrease in agricultural areas (<3000 ha) occurred in all provinces. While forest areas decreased in the west (Ordu) and east (Rize) of the basin, they increased in the central regions (Giresun, Trabzon). There was a decrease in natural vegetation except in Rize. The amount of this decrease is remarkable, especially for Trabzon (Senol 2019, Ustaoglu and Aydinoglu 2019).

It is understood that the comprehensive study for the Melet River shows similar characteristics to the basin trends in terms of land-use. Differently, it has been observed that the forested areas in the basin have been destroyed and the natural vegetation has increased. Flow data showed a decreasing trend in the east of the basin during the summer months; in the middle region between April and September, except for one station; and in the west, except for the January–March period at one station. As a result, considering the low flows in the summer months, there is an increase in the flows throughout the basin. In terms of land-use, the increase in residential and industrial area, and the decrease in agricultural and natural vegetation area, are factors that create or increase the severity of this effect. Unlike other regions, forest areas increase in the middle region of the basin. Decreases in flow values were observed in many months, especially at three of the four stations in this region. This decrease is thought to be caused by the change in climate and the increase in forest areas.

In trend analysis studies, the data length should be 30 years or more, especially to make climatic connections. In this study, the number of stations was limited to 14 due to insufficient

**Table 13.** Change in specified land-use types (ha) in the Eastern Black Sea Region (data from Senol 2019; Ustaoglu and Aydinoglu 2019).

| Region | Date range | Total area | Residential land | Industrial land | Agricultural land | Forest land | Natural vegetation land |
|---|---|---|---|---|---|---|---|
| Ordu | 1990–2012 | 586 100 | 1300–2300 | <500 | −3000 | −3000 | −3000 |
| Giresun | 1990–2012 | 702 500 | 500–1300 | <500 | −3000 | 500–10 000 | −3000 |
| Trabzon | 1990–2012 | 462 800 | 500–1300 | <500 | −3000 | 500–10 000 | −5000 |
| Rize | 1990–2012 | 383 500 | <500 | <500 | −3000 | −3000 | 0–500 |
| Melet Stream | 1990–2018 | 201 500 | 3570 | 350 | −1800 | −9730 | 4450 |

data lengths. Since inhomogeneity was detected in the data of three of these stations, the number of stations for trend analysis decreased to 11. For trend analysis, homogeneous datasets that do not have too much missing data and have not changed in terms of stations or measurement methods are needed. In addition, to represent the study area well, there should be a sufficient number of stations uniformly distributed in the basin. On the other hand, only how the mean flows change over time is evaluated with different trend methods. However, examining the minimum and maximum flows (seasonal, annual or daily), which is important in basin and water resources management, could not be done. Also, the effects of land-use change and/or climate change, together or separately, could not be studied in detail in this work. The general evaluation of trend methods is done without separating the flow data into high/low values in this study. Finally, the ranges of the flow data used in the study are not comparable due to the status of the stations. This situation has limited the observation of the changes at some stations in recent years.

In this study, the graphical methods proposed recently have advantages over other monotonic methods of trend analysis and how they should be applied and interpreted. In addition to the numerical values of monotonic trends, seasonal trend shifts in any basin, and large-scale hydrometeorological variables, graphical methods are indicators that are easy for decision makers to understand, and thus are helpful tools for water resources management. In particular, the IPTA method shows that the variations in the standard deviation and mean graphs within a calendar year are quite complex and irregular. However, the precipitation (which is one of the main factors of flow) regime in humid basins is more regular than that in semi-arid basins (Türkeş 2019). The complex shapes appearing in this humid basin indicate its tendency towards semi-arid basin characteristics (Nunes *et al.* 2008).

## 6 Conclusions

This study presents a homogeneity and trend analysis of monthly flow data for 14 streamgauge stations with a data length of more than 30 years selected from the Eastern Black Sea basin, Turkey. Homogeneity analyses of the annual mean flows in the scope of the study were carried out with a two-step approach. Stations D22A007, D22A052, and E22A032, which were determined to be inhomogeneous, were not included in the trend analysis. Trend analyses were made using Mann-Kendall test, seasonal Kendall test, ITST, and IPTA methods at 11 stations determined to have homogeneous data. In evaluating the results, while significant trends were mostly not determined according to the Mann-Kendall test, different trends were obtained with ITST and IPTA. Significant decreasing trends become prominent in the basin during the summer months (especially August). It is thought that the decreasing trends in the summer months may be due to the decrease in precipitation and effective evaporation. According to the results obtained from ITST and IPTA, the number of stations with increasing trends in autumn, winter and spring is higher than the number of stations with decreasing trends or no trends. Increasing trends were detected in autumn and spring, especially in the east of the basin. In the stations in the middle of the basin, decreasing trends were determined in the spring and summer months, except at one station. This decrease may be due to climate change and to the increase in forest area in the region. At station E22A045, located in the far west of the basin, decreasing trends in summer and autumn were observed. Also, the decreasing trends in flows at station E22A047, in the western part of the basin, in most months draw attention. When the results of three stations with observed trends for the seasonal Kendall test (increasing trend for D22A062 and E22A033; decreasing trend for E22A047) are compared with the Mann-Kendall test, there are some months with a trend similar to the seasonal Kendall test in the analysed months, but complete agreement was not observed.

The existence of both decreasing and increasing trends in different periods in the basin will cause irregular behaviour. This situation can bring water resource management difficulties, with (for example) water allocation, energy production efficiency determination of environmental flow amounts, flooding, and erosion caused by moist soil.

The fact that the trend detection rates of the ITST and IPTA are high and the results are mostly compatible with each other made them stand out compared to the Mann-Kendall test. In addition, in the Mann-Kendall test, the data should not have a serial dependency. This precondition is one of the disadvantages of the Mann-Kendall test. IPTA, which is one of the novel methods in the literature, provides information about the trend transition between consecutive parts of the time series as well as determining the trend in a series. As in this study, when the analysed parameter is studied with monthly data, it is possible to observe monthly and seasonal changes. In this way, transitions and imbalances between months can be detected and remarkable results can be obtained in water planning studies. Also, numerical and linguistic interpretations can be made over polygon templates in this method.

In this study, monthly mean flows were analysed. It will be useful to analyse daily, annual, and seasonal mean, minimum, and maximum flows in terms of water resources management in the basin. Within the scope of the study, the impact of climate change and land-use was evaluated in a general framework. Detailed examinations should be made with rainfall–runoff models to be created by taking into account the results obtained. Trend analysis should be repeated by increasing the number of stations. Finally, it is thought that it will be useful to divide the data into 10-year periods, analyse it using trend analysis methods, and determine the rate of change.

When the basin is examined in terms of vulnerabilities, approximately 10% of the installed power of hydroelectric power plants in Turkey is located in the EBSB. The decreasing trends in the summer months as a result of this study could negatively affect energy production. In addition, these results indicate that the basin is and/or may in future be adversely affected in terms of water allocation and water quality, especially in the summer months when the need for water is high. Finally, the effect of climate change on extreme values rather than average

values may cause flood events in the basin. It is known that the basin is very sensitive to floods.

## Acknowledgements

The authors thank the General Directorate of State Hydraulic Works for providing the flow data used in the study. Fatma Akçay is supported by a scholarship from the Technological Research Council of Turkey (TÜBİTAK) 2211-A Domestic Doctoral Scholarship Program and the Council of Higher Education 100/2000 Doctoral Scholarship Project.

## Disclosure statement

No potential conflict of interest was reported by the authors.

## ORCID

Fatma Akçay http://orcid.org/0000-0001-8129-3009
Murat Kankal http://orcid.org/0000-0003-0897-4742
Murat Şan http://orcid.org/0000-0001-7006-8340

## References

Ahmad, I., *et al*., 2018. Spatiotemporal analysis of precipitation variability in annual, seasonal and extreme values over upper Indus River basin. *Atmospheric Research*, 213, 346–360. doi:10.1016/j.atmosres.2018.06.019

Ahmed, N., *et al*., 2021. Changes in monthly streamflow in the Hindukush-Karakoram Himalaya Region of Pakistan using innovative polygon trend analysis. *Stochastic Environmental Research and Risk Assessment*. doi:10.1007/s00477-021-02067-0.

Alexandersson, H., 1986. A homogeneity test applied to precipitation data. *Journal of Climatology*, 6 (6), 661–675. doi:10.1002/joc.3370060607.

Ali, R., *et al*., 2019. Long-term trends and seasonality detection of the observed flow in Yangtze River using Mann-Kendall and Sen's innovative trend method. *Water*, 11 (9), 1855.

Alifujiang, Y., Abuduwaili, J., and Ge, Y., 2021. Trend analysis of annual and seasonal river runoff by using innovative trend analysis with significant test. *Water*, 13 (1). doi:10.3390/w13010095.

Almazroui, M., *et al*., 2019. Impacts of climate change on water engineering structures in Arid Regions: case studies in Turkey and Saudi Arabia. *Earth Systems and Environment*, 3 (1), 43–57. doi:10.1007/s41748-018-0082-6.

Ay, M., 2020. Trend and homogeneity analysis in temperature and rainfall series in western Black Sea region, Turkey. *Theoretical and Applied Climatology*, 139 (3–4), 837–848. doi:10.1007/s00704-019-03066-6.

Ay, M. and Kisi, O., 2015. Investigation of trend analysis of monthly total precipitation by an innovative method. *Theoretical and Applied Climatology*, 120 (3–4), 617–629. doi:10.1007/s00704-014-1198-8.

Ay, M. and Kişi, Ö., 2017. Trend analysis of streamflows at some gauging stations over the Kizilirmak River. *Teknik Dergi*, 28 (2), 7779. doi:10.18400/tekderg.304034.

Brown, A.E., *et al*., 2013. Impact of forest cover changes on annual streamflow and flow duration curves. *Journal of Hydrology*, 483, 39–50. doi:10.1016/j.jhydrol.2012.12.031

Buishand, T.A., 1982. Some methods for testing the homogeneity of rainfall records. *Journal of Hydrology*, 58 (1–2), 11–27. doi:10.1016/0022-1694(82)90066-X.

Caloiero, T., Coscarelli, R., and Ferrari, E., 2018. Application of the innovative trend analysis method for the trend analysis of rainfall anomalies in Southern Italy. *Water Resources Management*, 32 (15), 4971–4983. doi:10.1007/s11269-018-2117-z.

Ceribasi, G., Dogan, E., and Sonmez, O., 2013. Evaluation of sakarya river streamflow and sediment transport with rainfall using trend analysis. *Fresenius Environmental Bulletin*, 22 (3 A), 846–852.

Cigizoglu, H.K., Bayazit, M., and Önöz, B., 2005. Trends in the maximum, mean, and low flows of Turkish rivers. *Journal of Hydrometeorology*, 6 (3), 280–290. doi:10.1175/JHM412.1.

Costa, M.H., Botta, A., and Cardille, J.A., 2003. Effects of large-scale changes in land cover on the discharge of the Tocantins River, Southeastern Amazonia. *Journal of Hydrology*, 283 (1–4), 206–217. doi:10.1016/S0022-1694(03)00267-1.

Dabanlı, İ., *et al*., 2016. Trend assessment by the Innovative-Şen Method. *Water Resources Management*, 30 (14), 5193–5203. doi:10.1007/s11269-016-1478-4.

Diop, L., *et al*., 2018. Trend analysis of streamflow with different time scales : a case study of the upper Senegal River. *ISH Journal of Hydraulic Engineering*, 24 (1), 105–114. Taylor & Francis. doi:10.1080/09715010.2017.1333045.

Dogan, M., Ulke, A., and Cigizoglu, H.K., 2015. Trend direction changes of Turkish temperature series in the first half of 1990s. *Theoretical and Applied Climatology*, 121 (1–2), 23–39. doi:10.1007/s00704-014-1209-9.

Douglas, E.M., Vogel, R.M., and Kroll, C.N., 2000. Trends in floods and low flows in the United States: impact of spatial correlation. *Journal of Hydrology*, 240 (1–2), 90–105. doi:10.1016/S0022-1694(00)00336-X.

EPA (Environmental Protection Agency), 2011. Particulate Matter Emissions (1), 1–9. Available from: http://www2.cec.org/site/PPE/content/particulate-matter-emissions-0 [Accessed 23 Dec 2020].

Eris, E. and Agiralioglu, N., 2012. Homogeneity and trend analysis of hydrometeorological data of the Eastern Black Sea Region, Turkey. *Journal of Water Resource and Protection*, 4 (2), 99–105. doi:10.4236/jwarp.2012.42012.

Gajbhiye, S., *et al*., 2016. Trend analysis of rainfall time series for Sindh river basin in India. *Theoretical and Applied Climatology*, 125 (3–4), 593–608. doi:10.1007/s00704-015-1529-4.

GDM (General Directorate of Meteorology), 2020. Seasonal normals of the provinces. Available from: https://www.mgm.gov.tr/veridegerlendirme/il-ve-ilceler-istatistik.aspx [Accessed 20 Dec 2020].

Güçlü, Y.S., 2018. Alternative trend analysis: half time series methodology. *Water Resources Management*, 32 (7), 2489–2504. doi:10.1007/s11269-018-1942-4.

Güçlü, Y.S., Şişman, E., and Dabanlı, İ., 2020. Innovative triangular trend analysis. *Arabian Journal of Geosciences*, 13 (1). doi:10.1007/s12517-019-5048-y.

Gumus, V., 2019. Spatio-temporal precipitation and temperature trend analysis of the Seyhan–Ceyhan River Basins, Turkey. *Meteorological Applications*, 26 (3), 369–384. doi:10.1002/met.1768.

Hadi, S.J. and Tombul, M., 2018. Long-term spatiotemporal trend analysis of precipitation and temperature over Turkey. *Meteorological Applications*, 25 (3), 445–455. doi:10.1002/met.1712.

Haktanir, T. and Citakoglu, H., 2014. Trend, Independence, stationarity, and homogeneity tests on maximum rainfall series of standard durations recorded in Turkey. *Journal of Hydrologic Engineering*, 19 (9), 05014009. doi:10.1061/(ASCE)HE.1943-5584.0000973.

Helsel, D.R., *et al*., 2020. Statistical methods in water resources techniques and methods 4 – A3. *USGS Techniques and Methods*.

Huntington, T.G., 2006. Evidence for intensification of the global water cycle: review and synthesis. *Journal of Hydrology*, 319 (1–4), 83–95. doi:10.1016/j.jhydrol.2005.07.003.

IPCC (Intergovernmental Panel on Climate Change), 2007. Climate change 2007: impacts, adaptation and vulnerability. Contribution of Working Group II to the Fourth Assessment Report of the Intergovernmental Panel on Climate Change. Cambridge: Cambridge University Press.

IPCC, 2013. Climate change 2013: the physical science basis. Contribution of Working Group I to the Fifth Assessment Report of the Intergovernmental Panel on Climate Change [Stocker, T., F., D., Qin, G., K., Plattner, M., Tignor, S., K., Allen, J., Boschung, A., Nauels, Y., Xia, V., Bex ve P., M., Midgley (eds.)]. Cambridge, UK: Cambridge University Press, 1535.

Kahya, E. and Kalayci, S., 2004. Trend analysis of streamflow in Turkey. *Journal of Hydrology*, 289 (1–4), 128–144. doi:10.1016/j.jhydrol.2003.11.006.

Kalra, A., *et al*., 2017. Hydro-climatological changes in the Colorado River Basin over a century. *Hydrological Sciences Journal*, 62 (14), 2280–2296. Taylor & Francis. doi:10.1080/02626667.2017.1372855.

Kankal, M. and Akçay, F., 2019a. Investigation of hydroelectric energy situtaion in Eastern Black Sea Basin. *Omer Halisdemir University Journal of Engineering Sciences*, 8 (2), 892–901. (in Turkish). doi:10.28948/ngumuh.598239.

Kankal, M. and Akçay, F., 2019b. Trend analyses of precipitation of Trabzon Province, Northeastern Turkey. *Gümüşhane University Journal of Science and Technology Institute*, 9 (2), 318–331. (in Turkish). doi:10.17714/gumusfenbil.448542.

Karstarlı, Ç., *et al*., 2011. Analysis of hydroelectric potential in the Eastern Black Sea Basin. *2nd Water Struct. Symp*., 129–138. Diyarbakır, Turkey. (in Turkish)

Kendall, M., 1975. Rank correlation methods. Griffin, London.

Kişi, Ö., *et al*., 2018. Trend analysis of monthly streamflows using Şen's innovative trend method. *Geofizika*, 35 (1), 53–68. doi:10.15233/gfz.2018.35.3.

Kumar, S., *et al*., 2009. Streamflow trends in Indiana: effects of long term persistence, precipitation and subsurface drains. *Journal of Hydrology*, 374 (1–2), 171–183. doi:10.1016/j.jhydrol.2009.06.012.

Kundzewicz, Z.W., *et al*., 2008. The implications of projected climate change for freshwater resources and their management. *Hydrological Sciences Journal*, 53 (1), 3–10. doi:10.1623/hysj.53.1.3.

Li, Z., *et al*., 2009. Impacts of land use change and climate variability on hydrology in an agricultural catchment on the Loess Plateau of China. *Journal of Hydrology*, 377 (1–2), 35–42. Elsevier B.V. doi:10.1016/j.jhydrol.2009.08.007.

Mann, H.B., 1945. Nonparametric tests against trend. *Econometrica*, 13 (3), 245–259. doi:10.2307/1907187.

Meshram, S.G., *et al*., 2020. Long-term temperature trend analysis associated with agriculture crops. *Theoretical and Applied Climatology*, 140 (3–4), 1139–1159. doi:10.1007/s00704-020-03137-z.

Nemli, M.Ö., 2017. *Trend analysis of annual maximum rainfall intensity in Eastern Black Sea Region*. Thesis(MSc). Karadeniz Technical University. (in Turkish)

Nourani, V., *et al*., 2019. ANN-based statistical downscaling of climatic parameters using decision tree predictor screening method. *Theoretical and Applied Climatology*, 137 (3–4), 1729–1746. doi:10.1007/s00704-018-2686-z.

Nunes, J.P., Seixas, J., and Pacheco, N.R., 2008. Vulnerability of water resources, vegetation productivity and soil erosion to climate change in Mediterranean watersheds. *Hydrological Processes*, 22 (16), 3115–3134. doi:10.1002/hyp.6897.

Odemis, B. and Evrendilek, F., 2007. Monitoring water quality and quantity of national watersheds in Turkey. *Environmental Monitoring and Assessment*, 133 (1–3), 215–229. doi:10.1007/s10661-006-9574-1.

Onyutha, C., 2016. Identification of sub-trends from hydro-meteorological series. *Stochastic Environmental Research and Risk Assessment*, 30 (1), 189–205. Springer Berlin Heidelberg. doi:10.1007/s00477-015-1070-0.

Öztopal, A. and Şen, Z., 2017. Innovative trend methodology applications to precipitation records in Turkey. *Water Resources Management*, 31 (3), 727–737. doi:10.1007/s11269-016-1343-5.

Partal, T. and Kahya, E., 2006. Trend analysis in Turkish precipitation data. *Hydrological Processes*, 20 (9), 2011–2026. doi:10.1002/hyp.5993.

Pettitt, A.N., 1979. A non-parametric approach to the change-point problem. *Jstor*, 28 (2), 126–135. doi:10.1016/j.epsl.2008.06.016.

Rosner, A., Vogel, R.M., and Kirshen, P.H., 2014. A risk-based approach to flood management decisions in a nonstationary world. *Water Resources Research*, 50 (3), 1928–1942. doi:10.1002/2013WR014561.

Şan, M., *et al*., 2021. Innovative and polygonal trend analyses applications for rainfall data in Vietnam. *Theoretical and Applied Climatology*, 144 (3–4), 809–822. doi:10.1007/s00704-021-03574-4.

Sanikhani, H., *et al*., 2018. Trend analysis of rainfall pattern over the Central India during 1901–2010. *Arabian Journal of Geosciences*, 11 (15), 437. doi:10.1007/s12517-018-3800-3.

Saplıoğlu, K., Kilit, M., and Yavuz, B.K., 2014. Trend analysis of streams in the Western Mediterranean Basin of Turkey. *Fresenius Environmental Bulletin*, 23 (1 A), 313–324.

Satılmış, U., 2015. *A study on spatial and temporal variation of surface water quality in the stream Değirmendere* Watershed *(Trabzon)*. Thesis (MSc). Karadeniz Technical University.

Şen, Z., 2012. Innovative trend analysis methodology. *Journal of Hydrologic Engineering*, 17 (9), 1042–1046. doi:10.1061/(ASCE)HE.1943-5584.0000556.

Şen, Z., 2014. Trend identification simulation and application. *Journal of Hydrologic Engineering*, 19 (3), 635–642. doi:10.1061/(ASCE)HE.1943-5584.0000811.

Şen, Z., 2017. Innovative trend significance test and applications. *Theoretical and Applied Climatology*, 127 (3–4), 939–947. doi:10.1007/s00704-015-1681-x.

Şen, Z., 2018. Crossing trend analysis methodology and application for Turkish rainfall records. *Theoretical and Applied Climatology*, 131 (1–2), 285–293. doi:10.1007/s00704-016-1980-x.

Şen, Z., 2020. Water structures and climate change impact: a review. *Water Resources Management*, 34 (13), 4197–4216. doi:10.1007/s11269-020-02665-7.

Şen, Z., Şişman, E., and Dabanli, I., 2019. Innovative Polygon Trend Analysis (IPTA) and applications. *Journal of Hydrology*, 575 (May), 202–210. Elsevier. doi:10.1016/j.jhydrol.2019.05.028.

Senol, C., 2019. *Land use and spatial change in the Melet Stream Basin*. Thesis (PhD). Marmara University. (in Turkish)

Sezen, C. and Partal, T., 2020. Wavelet combined innovative trend analysis for precipitation data in the Euphrates-Tigris basin, Turkey. *Hydrological Sciences Journal*, 65 (11), 1909–1927. Taylor & Francis. doi:10.1080/02626667.2020.1784422.

Silva, R.M., *et al*., 2015. Rainfall and river flow trends using Mann–Kendall and Sen's slope estimator statistical tests in the Cobres River basin. *Natural Hazards*. doi:10.1007/s11069-015-1644-7.

Tan, M.L., *et al*., 2015. Impacts of land-use and climate variability on hydrological components in the Johor River basin, Malaysia. *Hydrological Sciences Journal*, 60 (5), 873–889. Taylor & Francis. doi:10.1080/02626667.2014.967246.

Topaloğlu, F., 2006. Trend detection of streamflow variables in Turkey. *Fresenius Environmental Bulletin*, 15 (7), 644–653.

Türkeş, M., 2019. *General climatology: fundamentals of atmosphere, weather, and climate*. Fourth ed. İstanbul: Kriter publisher.

Ustaoglu, E. and Aydinoglu, A.C., 2019. Regional variations of land-use development and land-use/cover change dynamics: a case study of Turkey. *Remote Sensing*, 11 (7), 1–33. doi:10.3390/RS11070885.

Uzlu, E., Akpınar, A., and Kömürcü, M.İ., 2011. Restructuring of Turkey's electricity market and the share of hydropower energy: the case of the Eastern Black Sea Basin. *Renewable Energy*, 36 (2), 676–688. doi:10.1016/j.renene.2010.08.012.

von Neumann, J., 1941. Distribution of the ratio of the mean square successive difference to the variance. *The Annals of Mathematical Statistics*, 12 (4), 367–395. doi:10.1214/aoms/1177731677.

Wei, X., Liu, W., and Zhou, P., 2013. Quantifying the relative contributions of forest change and climatic variability to hydrology in large watersheds: a critical review of research methods. *Water*, 5 (2), 728–746. doi:10.3390/w5020728.

Wijngaard, J.B., Klein Tank, A.M.G., and Können, G.P., 2003. Homogeneity of 20th century European daily temperature and precipitation series. *International Journal of Climatology*, 23 (6), 679–692. doi:10.1002/joc.906.

Wu, H. and Qian, H., 2017. Innovative trend analysis of annual and seasonal rainfall and extreme values in Shaanxi, China, since the 1950s. *International Journal of Climatology*, 37 (5), 2582–2592. doi:10.1002/joc.4866.

Yilmaz, M. and Tosunoglu, F., 2019. Trend assessment of annual instantaneous maximum flows in Turkey. *Hydrological Sciences Journal*, 64 (7), 820–834. Taylor & Francis. doi:10.1080/02626667.2019.1608996.

Yue, S., *et al*., 2002. The influence of autocorrelation on the ability to detect trend in hydrological series. *Hydrological Processes*, 16 (9), 1807–1829. doi:10.1002/hyp.1095.

Yüksek, Ö., Kankal, M., and Üçüncü, O., 2013. Assessment of big floods in the Eastern Black Sea Basin of Turkey. *Environmental Monitoring and Assessment*, 185 (1), 797–814. doi:10.1007/s10661-012-2592-2.

Zhang, Q., *et al*., 2008. Climate change or variability? The case of Yellow River as indicated by extreme maximum and minimum air temperature during 1960–2004. *Theoretical and Applied Climatology*, 93 (1–2), 35–43. doi:10.1007/s00704-007-0328-y.